12-1-2015

EFFECTS OF CONCRETE SLAB ON THE DUCTILITY, STRENGTH AND STIFFNESS OF STEEL MOMENT FRAMES WITH REDUCED BEAM SECTION CONNECTIONS

Sanchit Poudel
Southern Illinois University Carbondale, sanchitpoudel@siu.edu

EFFECTS OF CONCRETE SLAB ON THE DUCTILITY, STRENGTH AND STIFFNESS OF STEEL MOMENT FRAMES WITH REDUCED BEAM SECTION CONNECTIONS

by

Sanchit Poudel

B.E., Pulchowk Engineering Campus, 2012

A Thesis
Submitted in Partial Fulfillment of the Requirements for the
Master of Science Degree

Department of Civil and Environmental Engineering
in the Graduate School
Southern Illinois University Carbondale
December 2015

THESIS APPROVAL

EFFECTS OF CONCRETE SLAB ON THE DUCTILITY, STRENGTH AND STIFFNESS OF STEEL MOMENT FRAMES WITH REDUCED BEAM SECTION CONNECTIONS

By

Sanchit Poudel

A Thesis

Submitted in Partial Fulfillment of the Requirements for the Degree of

Master of Science

in the field of Civil Engineering

Approved by:

Dr. J. Kent Hsiao, Chair

Dr. Aslam Kassimali

Dr. Jale Tezcan

Graduate School

Southern Illinois University Carbondale

November 3, 2015

AN ABSTRACT OF THE THESIS OF

SANCHIT POUDEL, for the Master of Science degree in CIVIL ENGINEERING, presented on November 3, 2015, at Southern Illinois University Carbondale

TITLE: EFFECTS OF CONCRETE SLAB ON THE DUCTILITY, STRENGTH AND STIFFNESS OF STEEL MOMENT FRAMES WITH REDUCED BEAM SECTION CONNECTIONS

MAJOR PROFESSOR: Dr. J. Kent Hsiao

It was not thought that there would be some major flaws in the design of widely used steel moment frames until the Northridge Earthquake hit the California on January 17, 1994. Until then, steel moment frames were practiced as the most ductile system and were used in buildings from few stories to skyscrapers. The heavy devastation from Northridge Earthquake was an alarm for all the people related to the design and construction of such structures and pushed everybody to act fast to find some possible solutions to such never-expected-problems.

Following the earthquake, FEMA entered into a cooperative agreement with the SAC joint venture in order to get a transparent picture of the problems in the seismic performance of steel moment frames and to come up with suitable recommendations. The research was specifically done to address the following things: to inspect the earthquake-affected buildings in order to determine the damage incurred in the buildings, to find out ways to repair the damaged buildings and upgrade the performance of existing buildings, and to modify the design of new buildings in order to make them more reliable for seismic performance. Among the various new

design suggestions, the Reduced Beam Section (RBS) connection has been one of the most efficient and reliable option for high ductility demands.

The purpose of this research was to study the behavior of concrete slabs in the performance of steel moment frames with reduced beam sections based on ductility, strength and stiffness. The slab is an integral part of a building. It is always wiser to consider the slab in order to assess accurately the seismic behavior of a building under the earthquake loading. In this research, two sets of finite element models were analyzed. Each set had one bare steel moment frame and one concrete slab frame which acted as a composite section.

The connections were designed using the AISC Seismic Design manual (AISC 2012). The finite element modeling was done using NISA DISPLAY-IV (NISA 2010). All the models, with and without the slab were analyzed under the same boundary conditions and loads. Both non-linear and linear analyses were performed. The results from non-linear analysis were used to compare the ductility and strength whereas linear analysis results were used to compare the stiffness between bare steel and composite frame models.

ACKNOWLEDGMENTS

I am greatly indebted to my academic advisor Dr. J. Kent Hsiao for his continuous guidance and all his support at every stage: from selecting the thesis topic, conducting the research using finite element software and successfully preparing the thesis.

I would like to express my appreciation and gratitude to the committee members Dr. Aslam Kassimali and Dr. Jale Tezcan for agreeing to be a part of my graduate committee and providing assistance throughout the MS program.

I am very thankful to the Department of Civil and Environmental Engineering for providing me the golden opportunity to complete my graduate program, and department chair Dr. Sanjeev Kumar for all his care and support. Additionally, I would like to thank office manager, Tuesday L. Ashner, for helping me with paperwork and continually giving suggestions during my time in the department. Also, I would like to thank all my friends, classmates, roommates, and all other teachers and faculty members who directly or indirectly helped me achieve my goal.

Last, but not the least. I would like to thank my family members for all their love, support and encouragement. Without their support, I would never have been where I am today.

TABLE OF CONTENTS

LIST OF TABLES

TABLE PAGE

LIST OF FIGURES

FIGURE PAGE

CHAPTER 1

INTRODUCTION

The Northridge Earthquake in 1994 changed the generally accepted notion of engineers and fabricators that the welded steel moment frame building is the most ductile moment resisting frame. Following that earthquake, a number of steel moment-frame buildings were found to have experienced brittle fractures of beam-to-column connections (FEMA-350, 2000) . The reduction in previously assumed adequacy in connection ductility, strength and stiffness of the lateral frame raised serious tension regarding the inspection of affected buildings, assessment of their residual strength and stiffness, finding of suitable retrofitting measures, and examination of the potential vulnerabilities of the existing buildings in the seismically active areas (Iwankiw, 2004).

Following the earthquake, wide ranges of research are going on to find the most efficient solutions to the problems in order to avoid any possible future damage. Over the last two decades, the design professionals and construction industries have come up together hand in hand to review, study, and revise different parameters involved in the construction of steel moment frames. Various research carried out by AISC in collaboration with different organizations and the FEMA-SAC program have shed light on the improvements in design, fabrication, and workmanship which are expected to account for an increased seismic performance of steel moment frames (Iwankiw, 2004).

The post-earthquake research suggested two solutions to the problems. One is to reinforce the beam column connections with the use of flange cover plates, ribs, haunches, side plates etc. Another is the weakening of the section of the beam away from the face of the columns known as the “Dogbone” moment connection or Reduced Beam Section connection (Civjan et al., 2000; Engelhardt et al., 1996; Park and Hwang, 2003). The reduction in cross

sectional area reduces the moment capacity at that location of the beams, where yielding will be concentrated at the reduced sections, and ultimately protecting the connections from brittle fracture (Sophianopoulos and Deri, 2011). The weakening method avoids the higher stress generation on the supporting columns, reduces the weld-metal volume, and decreases supplementary material requirements which makes it more reliable and economic (Iwankiw, 2004; Park and Hwang, 2003). The scope of this research is limited to the use of radius cut reduced beam section.

A distinguished feature of reduced beam section is that portions of beam flange are trimmed away in the region adjacent to the beam-column connection. The RBS forces the yielding and hinge formation away from the beam column connection to form at the reduced section of beam limiting the moment that can be developed at the face of column. The Dogbone enhances the ductility of the system significantly with a small reduction in the strength and stiffness of a frame. Thus, this trading of small amount of strength for a large increase in ductility is seen as an excellent bargain for seismic resistant buildings (Engelhardt et al., 1996).

The use of slabs in the steel moment frames as a composite beam has been a common practice all over the world. So, with the overwhelmingly increasing popularity of RBS, it was deemed necessary to study the effect of composite slabs on the structures so that accurate assessment can be made of the seismic demand in structures considering the dead and live load coming from the slabs.

To ensure the acceptable seismic performance of steel moment frames, it is necessary to have adequate combination of stiffness, strength and ductility. It has always been a topic of interest to study whether the composite slabs would act to help improve the seismic performance in steel moment frames or further make the frames more vulnerable to the seismic force.

The scope of this research was to study the effect of composite slab on steel moment frames employing radius cut Reduced Beam Sections, and comparison was done with bare steel specimen frames based on their stiffness, strength and ductility. The connection was designed using AISC Seismic Design Manual (AISC 2012). The modeling and analysis of the frame was performed with the help of finite element software NISA DISPLAY-IV (NISA 2010). A partial frame of multi-story moment frame was used for the analysis. Two sets of models were designed and each set consists of one bare steel frame and one composite slab frame. The span, height, and boundary conditions are kept same for all the models. The ductility, strength and stiffness of each model were calculated, and comparison was done to see the effect of composite slabs.

CHAPTER 2

LITERATURE REVIEW

2.1 Background of Steel Moment Frame

Steel moment frame buildings are designed with the basic intent to resist earthquake damage based on the ground that they are capable of extensive yielding and plastic deformation, without loss of strength. Damage in these structures was expected to be due to moderate yielding and localized buckling of the steel. However, the post-Northridge earthquake observation indicated a lot of brittle fractures within the connections at very low levels of plastic demand, and in some cases, while the structures remained essentially elastic (FEMA-350, 2000).

The basic purpose of steel moment frames is to resist moments caused by lateral forces by achieving high ductility through yielding, and be capable of remaining intact through several cycles of inelastic rotations due to seismic loading. The advantage of using moment frames is the availability of more space which provides more architectural freedom in design. On one hand, the connections for steel moment frames increases the price of project by being labor intensive compared to shear wall structures. However, on the other hand, lesser forces imposed by these frames on the foundation results in somewhat economical foundation system (Hamburger et al., 2009). Figure 2.1.1 shows a typical moment resisting frame.

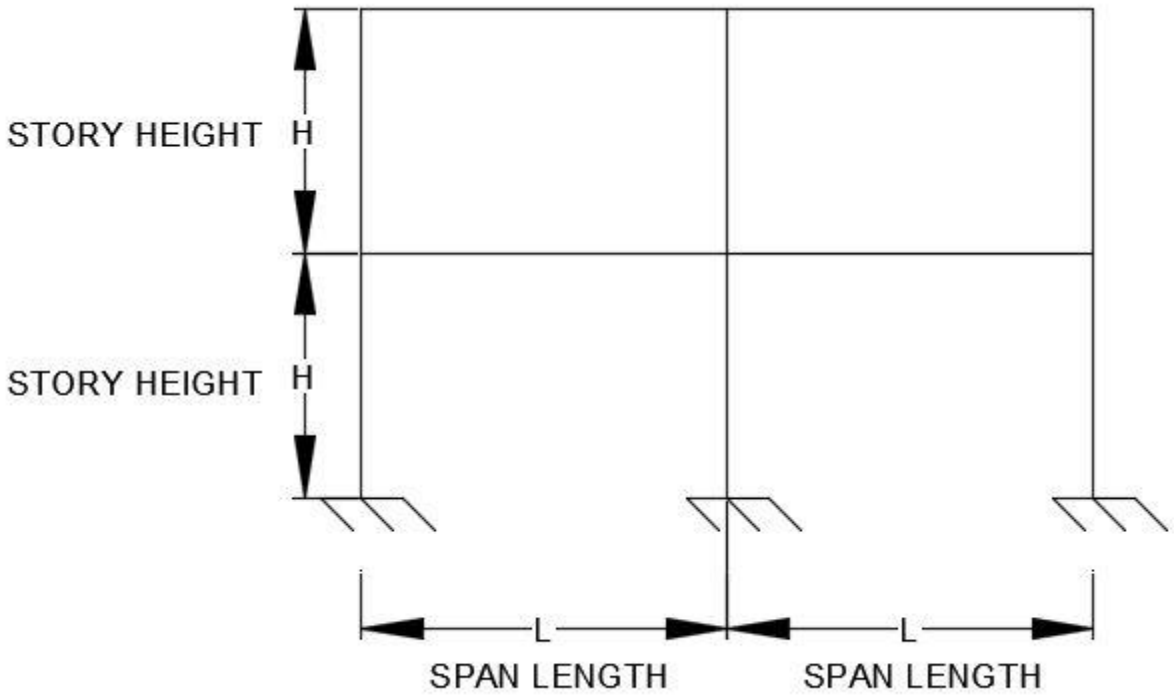

Figure 2.1.1:Typical Moment Resisting Frame

The use of steel moment frames in building construction initiated with the Home Insurance Building in Chicago, a 10-story structure constructed in 1884 with a height of 138 feet, was often called as the first skyscraper (Hamburger et al., 2009). After this, there was a rapid increase in the use of steel moment frames in the construction of high rise buildings and various modifications in the construction practices to make them safer seismically. Basically, there are three types of moment resisting frames: 1) Ordinary Moment Frame (OMF), 2) Intermediate Moment Frame (IMF) and, 3) Special Moment Frame (SMF).

OMFs will normally be more rigid than IMFs or SMFs, but can have much poorer inelastic response characteristics. OMFs are able to resist the onset of damage due to stronger levels of ground shaking than the other moment frames. But, as the ground intensity increases, OMFs possesses a much greater risk of collapse than IMFs, which possesses more risk than

SMFs. So, the proper use of various moment frames depends on the various parameters that include height of structure, usage of structure, seismic vulnerability of the site, etc. In spite of defining more restrictive design force and drift criteria to limit the amount of inelastic demand these IMFs may experience, decision was made to omit this IMF system from the building code (FEMA-350, 2000).

SMF structures are expected to be able to dissipate an extensive amount of energy by the formation of plastic hinges. The term "special" was adopted because their design involved special criteria and they were expected to demonstrate superior performance in times of strong earthquakes (Hamburger et al., 2009). It was only after the Northridge Earthquake, the design defects in those moment frames came to light. A large number of steel moment frames experienced brittle failure of welded beam-to-column connections that included fractures in the bottom beam flange-to-column flange complete-joint penetration groove welds, cracks in beam flanges, and cracks through the column sections (Hamburger et al., 2009).

After that earthquake, FEMA and SAC entered into the contractual agreement where they did extensive research on steel moment frames to find out the actual cause of failure and propose some measures to avoid future such disaster. All the different solutions suggested after the careful investigations of the damages can be classified as either the strengthening types or the weakening types (Chen et al., 2001). The purpose of all these design modifications were to avoid the brittle failure of beam-column connections by moving the plastic hinge away from the face of the columns and reducing the stress levels in the vicinity of the complete joint penetration (CJP) flange welds. The connection strength can be increased by using one of these: cover plates, triangular haunches, straight haunches, upstanding ribs, lengthened ribs, and side plates. Similarly, weakening can be done either by cutting a portion of beam flange (reduced beam

section connections) or the beam web (wedge beam connections) and reduced beam web connections (Hedayat and Celikag, 2009). The strengthening method was superseded by the weakening method for being more uneconomical and time consuming. Among various weakening methods, this research focuses on the most popular and widely used Reduced Beam Section (RBS) connections.

2.2 Reduced Beam Section

The concept of using RBS goes to European research Plumier, who developed an idea of creating locally weak zone away from the beam column connection so that plastic hinging can take place at the desired location. This novice idea was actually a by-product of limited experiments with small European shapes, patented by the late European steel producer S. A. Arbed ("Antiseismic steel structural work", U.S. Patent No. 148, 642, 1992). Arbed generously waived the commercial rights for its broad public use in United States (Iwankiw, 2004). Since then, a lot of research has been done to find the best possible shape of reduced beam section.

A lot of research had been carried out to study the most effective shape of reduced beam section. Investigations were mainly focused to compare the results among the three different types: tapered cut, radius cut, and straight cut connections. Figure 2.2.1 shows different Dogbone cutouts. Test results have shown radius cut to be the most superior and straight cut to be the most inferior connection (Englehardt et al., 1997; Jin and El-Tawil, 2005; Jones et al., 2002). Also, Radius cut RBS came out to be most popular because it was relatively easy to fabricate, and it avoided stress concentration at the reentrant corners as seen in straight cut and tapered cut section (Lee and Chung, 2007). In this research also, radius cut connection is employed for more effective and efficient result.

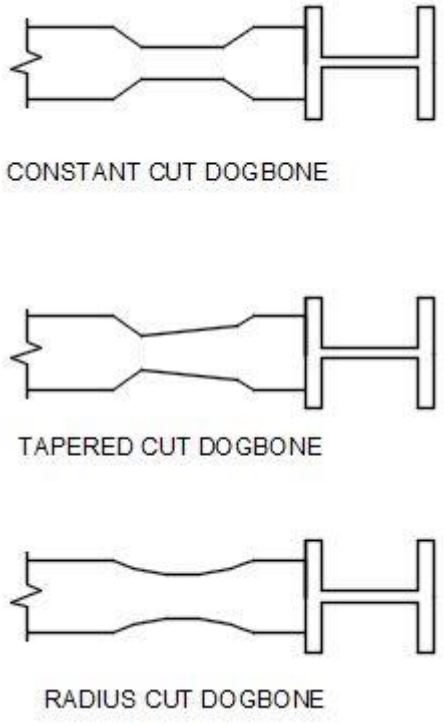

Figure 2.2.1: Different Dogbone cutouts

In the Reduced beam Section connection also called as “Dogbone connection”, the flanges are selectively trimmed in both the top and bottom flanges near the beam-to-column connection to reduce the cross sectional area of the beam. Figure 2.2.2 shows a typical circular cut RBS. The RBS forces yielding and hinge formation to occur within the reduced portion and limits the moment that can be formed at the face of the column. Although, the RBS essentially weakens the beam, its impact on the overall lateral strength and stiffness of a steel moment frame is generally small. However, it significantly enhances the ductility of the frame (Han et al., 2009; Jones et al., 2002; Moore et al.,1999). A number of research carried out on RBS indicates the connection to be one of the most promising concepts for the design of ductile steel moment frames for severe seismic applications capable of providing a high level of performance and good economy (Englehardt et al., 1997).

An experimental investigation was carried out on seismic resistant steel moment connections using a reduced beam section where portions of the beam flanges near the beam-column connection were trimmed in order to enhance ductility under severe seismic loads. It was seen that the average reduction in stiffness for a 50 percent flange reduction was on the order of 6 to 7 percent. Similarly, for a 40 percent flange reduction, the stiffness was reduced by 4 to 5 percent. From the observation, the radius cut Dogbone connection appears to provide a high level of performance and good economy (Englehardt et al., 1997).

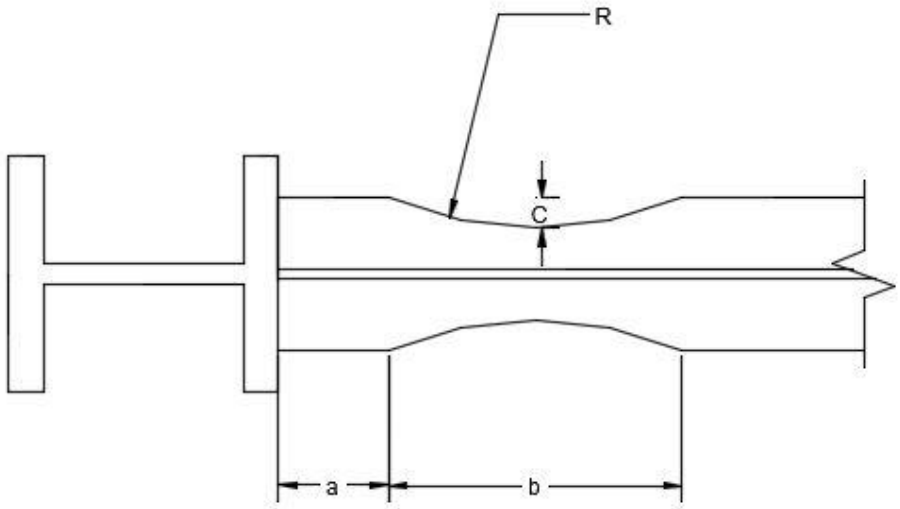

Figure 2.2.2: Dimension of the circular cut RBS

Where,

$a \approx (0.5 \text{ to } 0.75) \times b_f$

$b \approx (0.65 \text{ to } 0.85) \times d_b$

$c \approx (0.1 \text{ to } 0.25) \times b_f$

$R = \frac{4c^2 + b^2}{8c}$

b_f= width of beam flange

d_b= depth of beam

2.3 Effects of Plastic Hinge on Ductility, Strength and Stiffness

Strength, stiffness, and ductility are the major attributes affecting the seismic performance of steel moment frame connections, and it is seen that they are controlled by yield mechanisms and failure modes. The yield mechanism introduces plastic deformation which ultimately reduces the connection stiffness and these changes are necessary as they help to access the performance of the connection in the earthquake. Similarly, failure modes lead to the fracture, tearing, or deterioration of connection performance which ultimately limits the connection ductility and resistance. Ductility is measured by the plastic rotational capacity of the connection. Ductility is assured by making sure than the yield mechanism resistance is significantly less than critical failure mode resistance (Roeder, 2002a, 2002b).

Steel moment frames are anticipated to develop their ductility by going through significant inelastic behavior in numerous members when exposed to severe seismic shaking. And, this inelastic behavior is expected to occur in the form of plastic hinging in the beams, adjacent to the beam-column connections. The hinging should occur over multiple stories in order to spread the total displacement demand and limit the local deformation and member strains to a level that the members can withstand in a properly designed system. The ideal plastic hinge formation in the frame is shown in Figure 2.3.1. In addition to this, inelastic behavior can be expected to occur in beam-column joint panel zones and at column bases (Hamburger et al., 2009). However, it is always undesirable to form plastic hinge in the column as the column failure is more serious than the failure of unimproved connections since it is more likely to lead to a collapse mechanism.

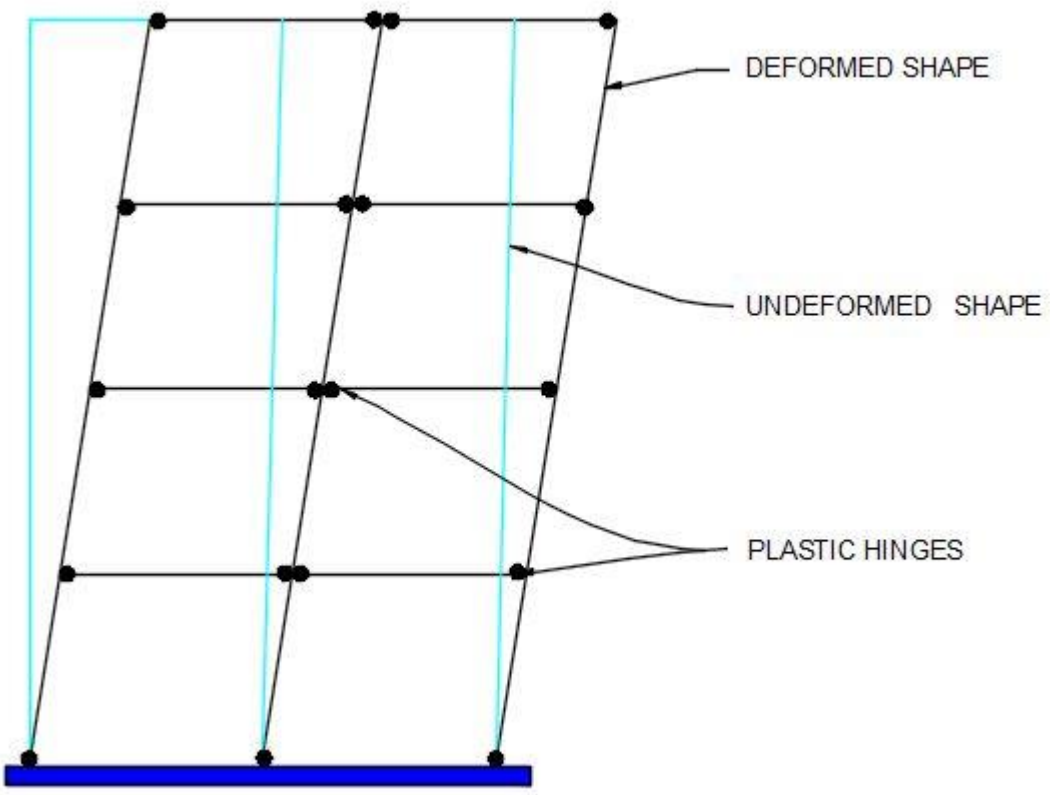

Figure 2.3.1: Idealized mechanism for strong column weak beam design

In this research, more effort is given to form the plastic hinges in the reduced section of beam and control the failure mechanism. In the study, two types of steel moment frames - composite slab frame and bare steel frame - are used to compare the ductility, strength and stiffness of the frames to investigate the effect of composite slab in the performance of steel moment resisting frames.

2.4 Use of Steel- Concrete Composite System

It can be seen that almost all steel moment frames are supplemented with concrete slabs. The Steel-concrete composite system is widely used because of benefits of combining the two materials. Reinforced concrete is inexpensive, massive, and stiff, while steel member are strong, lightweight, and easy to assemble (Spacone and El-Tawil, 2004). In common construction of

buildings, concrete slab is almost always present. So, it is of immense necessity to study the effect of slabs on the steel moment frames.

Neglecting the slabs composite effect in the structures may result in inappropriate design. There could be difference in the estimation of stress values generated in the frames as well as the deformation that takes place in the structures. The presence of composite slabs could play some role to alter the behavior of plastic hinges formation and the desired concept of strong column weak beam moment frame connections. In almost all the construction, slabs are the inseparable part of the frames.

Jones, Fry, and Engelhardt (Jones et al., 2002) performed a full scale test on eight samples of interior joint with reduced beam section connection to study the effect of composite slab on the frame. Each specimen was subjected to a standard quasi-static cyclic load and seven out of eight specimens achieved total elastic plus plastic story drift ratios. From the experiment, the presence of slab proved to be beneficial to the beam performance by enhancing the beam stability and delaying the strength degradation. The presence of slab appeared to stabilize the beam against lateral torsional buckling. And, no special treatment was needed for the slab, such as leaving a gap between the slab and the face of the column.

Civjan, Engelhardt, and Gross (Civjan et al., 2001) performed tests on full-sized interior sub-assemblages where the specimen were loaded at column tip under quasi-static cyclic loading to study the effect of composite slab on the frame. From the experiment, it was observed that the composite specimen developed larger plastic rotations and larger moments as compared to bare steel specimen. This result suggests a potentially beneficial effect of the slab that includes improved resistance to local and lateral instabilities of the beam with slight increase in elastic stiffness and strength over bare steel specimen.

Also, Zhang and Ricles (Zhang and Ricles, 2006) performed an experimental investigation of seismic behavior of RBS moment connections. Five of his six full scale specimen consisted of a composite floor slab. From the study, it was concluded that the composite floor slab developed a greater increase in strength relative to the bare steel beam. The lateral restraint provided by the floor slab enhanced the connection performance by reducing the strength degradation due to lateral buckling of the beam.

The objective of this research is to use finite element analysis to study and compare bare steel frames with composite slab frames based on grounds of ductility, strength and stiffness.

CHAPTER 3

PROCESSES AND MODELING

3.1 Introduction

A partial frame of a multistory single-bay moment frame was considered for this research. The partial frame concept can be used in this condition since it is assumed that there is no bending moment at the mid height of the column due to lateral loads. Two Reduced Beam Sections was employed close to the ends of the beam as shown in Figure 3.1.1 to see the real picture of mode of generation of plastic hinge in the reduced part and the effect of those hinges on the overall stability of SMFs. Two sets of models were analyzed. Each set having one composite slab frame and one bare steel frame. Beam and column were designed to satisfy strong-column-weak-beam criteria in order to force formation on plastic hinge within the beam and control the failure mechanism. The boundary condition, load, span and height of the frame were kept typical for each set of models with and without composite slab as shown in Figure 3.1.1, Figure 3.1.2, Figure 3.1.3, and Figure 3.1.4. To meet the intended objective of performing the research, the vertical load was kept constant whereas the lateral load was applied with 100 time steps increments.

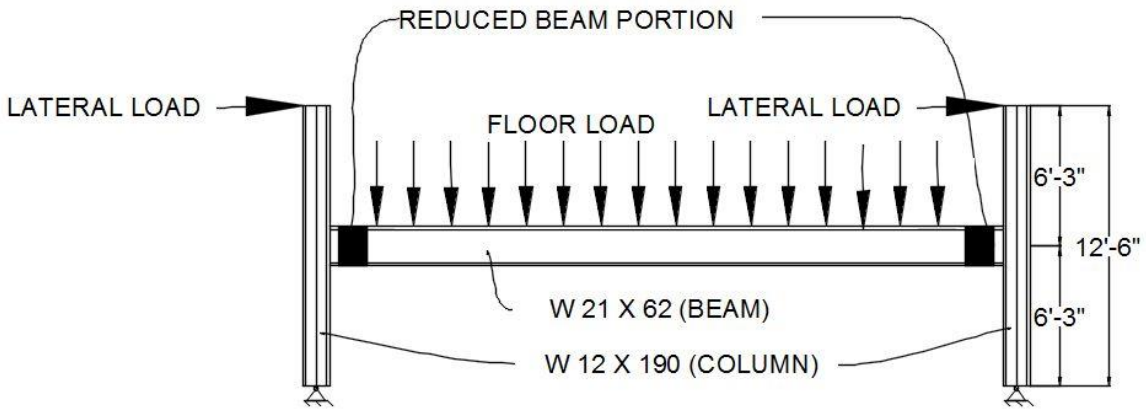

Figure 3.1.1: Bare Steel Frame (Model 1a)

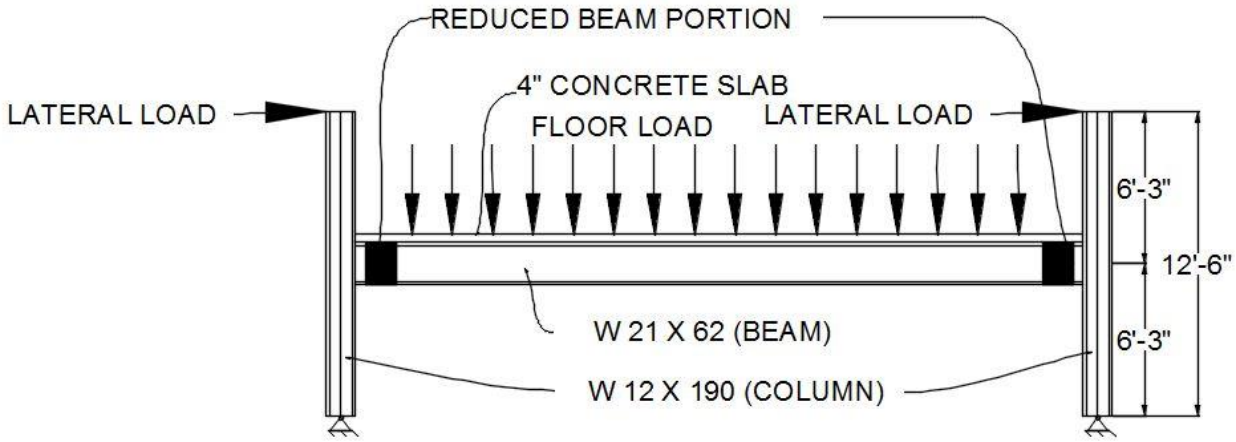

Figure 3.1.2: Composite slab frame (Model 1b)

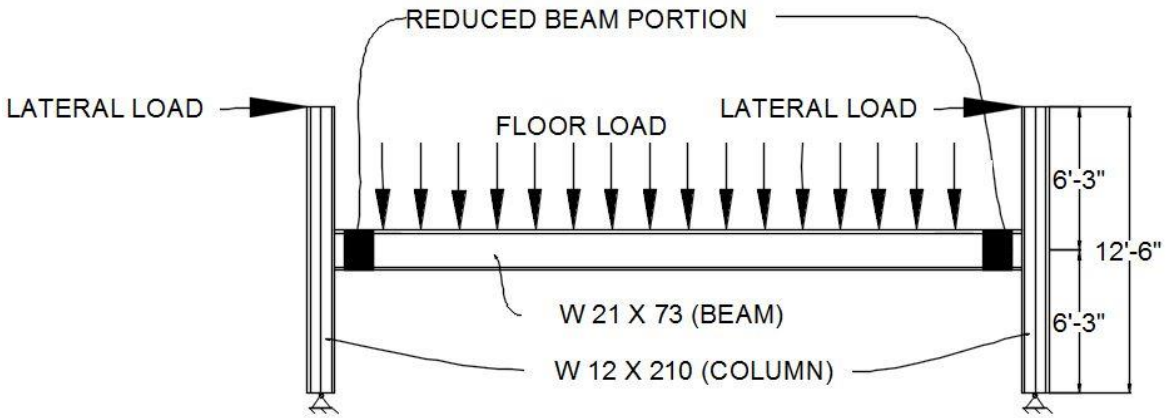

Figure 3.1.3: Bare Steel Frame (Model 2a)

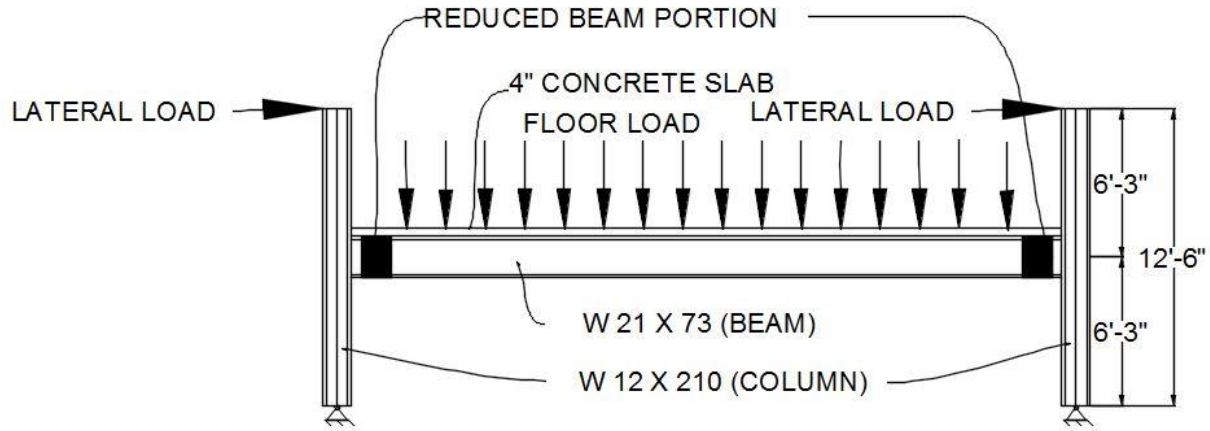

Figure 3.1.4: Composite slab frame (Model 2b)

3.2 Model Geometry

The Reduced Beam Sections were designed using AISC Seismic Design Manual (AISC 2012). The frame configuration is 30 feet long and 12.5 feet high. And, the width of slab is taken to be 25 feet. For model 1a and 1b, the beam used in the analysis is W 21×62 and the column used is W 12×190. Similarly, for model 2a and 2b, the beam is W 21×73 and column is W 12×210. Pinned supports are used at the column base since the minimum bending moment is

close to zero at the mid-height of the column in each story due to lateral loads. The design process showed none of the models required continuity or doubler plates for more stability.

3.3 Material Properties

The steel used for the connection design is A992. The true stress strain curve for A992 is shown in Figure 3.3.1 (Bartlett et al., 2001). The Modulus of Elasticity used is 29000 ksi with a Poisson's ratio of 0.3. Also, the yield strength of the material used in the analysis is 57 ksi and the fracture strength is 84 ksi. The yield strength of material refers to the point of formation of plastic hinge in the frame whereas fracture strength refers to the point at which the frame fractures and becomes no more useful as a load bearing structure.

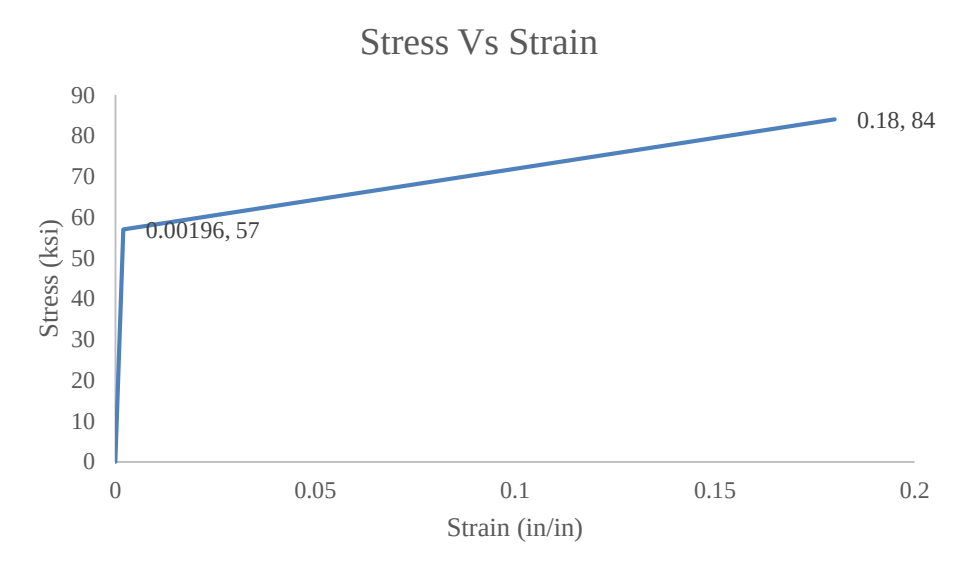

Figure 3.3.1: True Stress- Strain Curve for A992 Steel

Table 3.3-1: Stress- Strain data used in the analysis for A992 steel

Stress (ksi)	Strain (in/in)
0	0
57	0.00196
84	0.18

The composite slab was also used in each model type for the composite action. The Modulus of Elasticity used for the concrete is 3640 ksi and Poisson's ratio is 0.2. The fracture stress for the concrete is 4 ksi with strain value of 0.002 (Wang et al., 2007). Since, concrete is weak is tension and does not provide significant support to the frame, the concrete slab was used only in the compression zone in the design of frame for analysis.

The concrete slab acts as a composite slab over the steel frames. For the analysis, strength of frame was taken to be the one at which the steel frame fractured, and the cracks developed at the face of the column was ignored.

3.4 Loads and Boundary Conditions

After designing frames and defining material properties, loads were applied. Lateral loads were applied at the tops of the columns as shown in the Figure 3.1.1, 3.1.2, 3.1.3 and 3.1.4. The lateral loads were applied at the column web to effectively transfer the load uniformly all over the structure. The lateral loads were applied for 100 time steps. The time steps indicate the ratio of increment of the load.

Similarly, floor loads were applied along the top of the web of the beam since web is more rigid. The floor loads were applied as a constant load in the analysis. All the loads were applied as a pressure load for even stress distribution.

The boundary conditions were kept same for each set of model. The column bases were pinned and were kept movement restrained in x, y and z direction. Figure 3.4.1 shows typical full frame with loads and boundary conditions. Similarly, Figure 3.4.2 and Figure 3.4.3 shows enlarged view of bare steel frame and composite slab frame respectively with loads and boundary conditions.

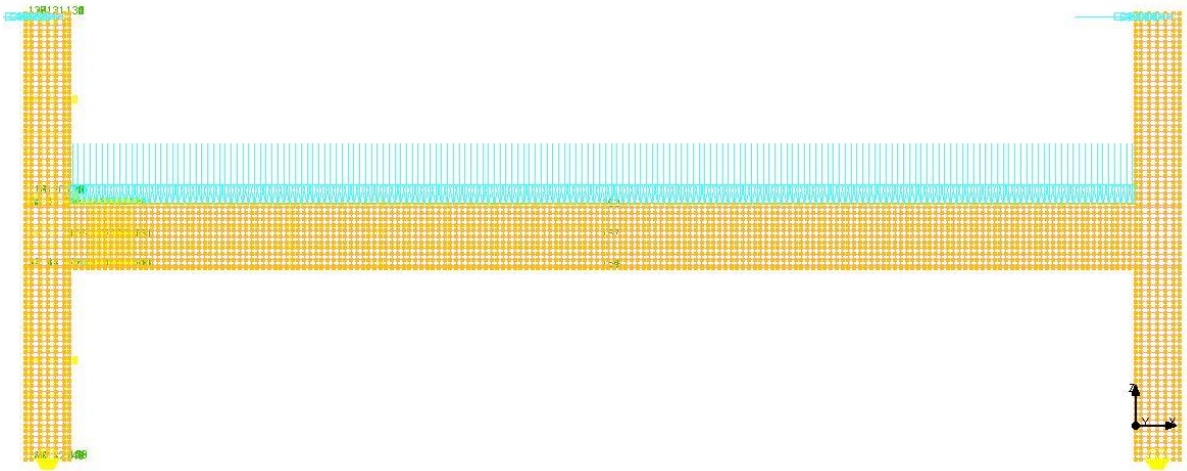

Figure 3.4.1:Typical full frame with loads and boundary conditions

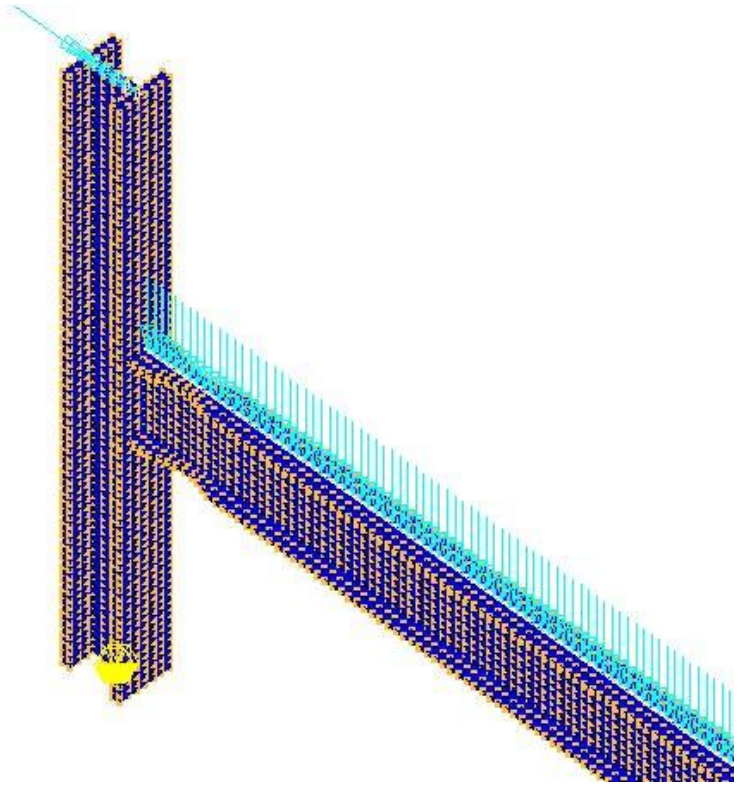

Figure 3.4.2: Enlarged view of bare steel frame with loads and boundary conditions

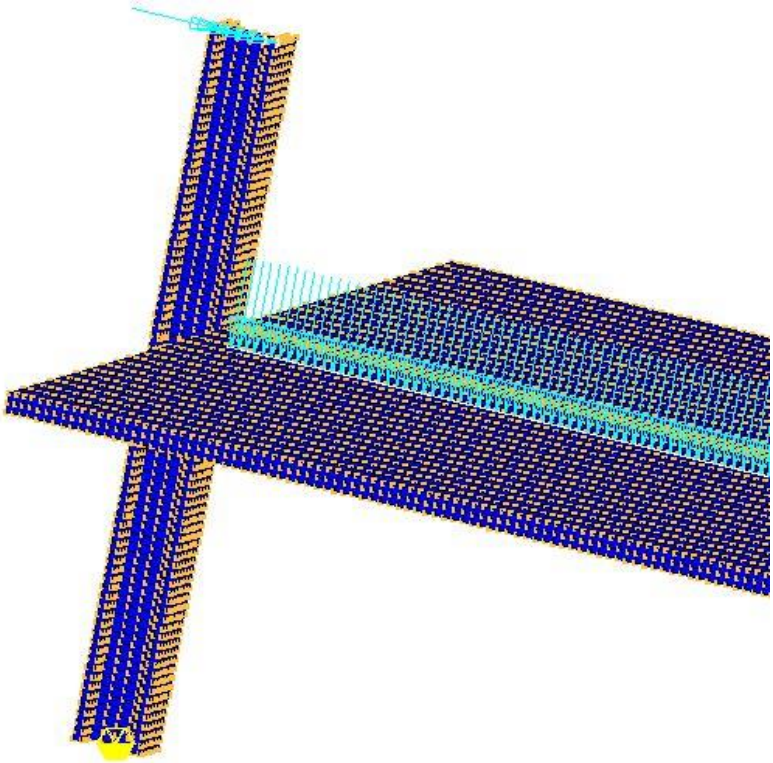

Figure 3.4.3: Enlarged view of composite slab frame with loads and boundary conditions

3.5 Analysis with NISA

The models were analyzed using finite element software NISA DISPLAY-IV (NISA-2010). The models were composed of many small elements for the accurate assessment of stress variation in the areas of high stress concentration. Nonlinear analyses were performed to observe the nature of plastic hinge formation.

The models were run for 100 time steps using the finite element analysis software. For each model, the Von-Mises stress and 1st Principal stress were observed. The Von-Mises stress is related to the formation of plastic hinges in the frame. The 1st Principal stress is related to the fracture of the structural elements. Referring to Figure 3.3.1, the true stress-strain curve for A992 steel, the yielding stress is 57 ksi and the ultimate stress is 84 ksi.

Both linear and nonlinear analyses were performed in this research to compare the stiffness, ductility and strength of bare steel frames with that of composite slab frames. From the non-linear analysis, the maximum lateral displacement of the frames was observed and ductility of the frame was calculated. Similarly, linear analysis was performed to calculate stiffness of the frame. Then, comparison was made between the bare steel frames and composite slab frames in terms of ductility, strength and stiffness.

CHAPTER 4

RESULTS AND DISCUSSIONS

4.1 Introduction

All of the results obtained from the finite element analysis are summarized in this chapter. The frames were designed using AISC Seismic Design Manual and then models were created and analyzed using NISA DISPLAY IV. All the models were analyzed linearly and nonlinearly, and displacements were observed for the calculation of ductility and stiffness. Lateral loads were applied at the free ends of the columns. Floor loads were applied as a pressure load on the beam web throughout the length of the beam. Also, pinned connection was assumed at the base of both columns.

The formation of plastic hinges in the Reduced Beam Sections is the most desirable trait in this research. Since the beam is modeled with two reduced sections, the goal is to create hinges at both the reduced sections. The determination of plastic hinge formation was done by observing the Von-Mises stress distribution in the beam. The yielding of beam is said to occur if the stress exceeds 57 ksi. An example of plastic hinges formed in the frame is shown in Figure 4.1.1.

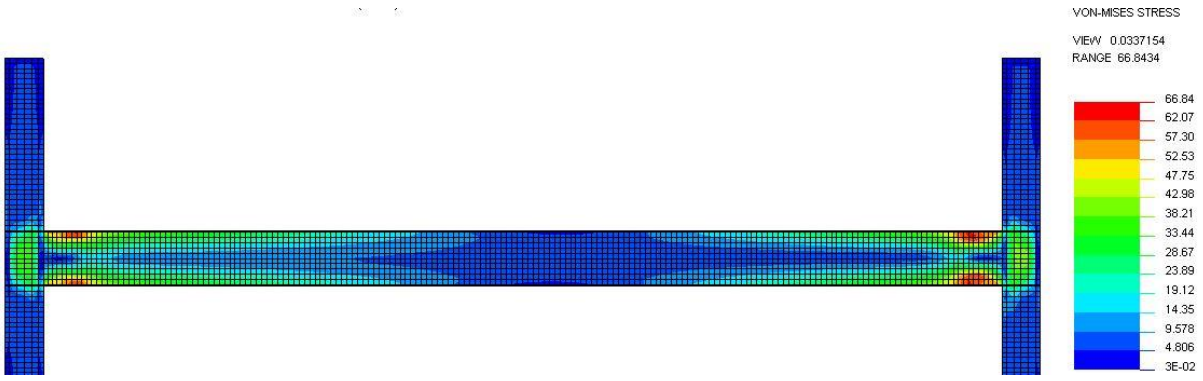

Figure 4.1.1: Formation of Plastic hinge on both RBS

4.2 Bare steel frame

For both the bare steel models, 1st Principal stress and Von-Mises stress was observed. In the model 1a, as shown in Figure 4.2.1 and Figure 4.2.2, 1st Principal stress reached 69.55 ksi and Von-Mises stress reached 66.84 ksi respectively at time step 64 (The last step at which the 1st Principal stress is less than 84 ksi). Figure 4.2.2 shows that the yielding Von-Mises stress has entered the web causing the formation of plastic hinge in the reduced section which is the desired result. Similarly, Figure 4.2.3 represents the Von-Mises stress reaching yield value of 57.30 ksi at time step 44.

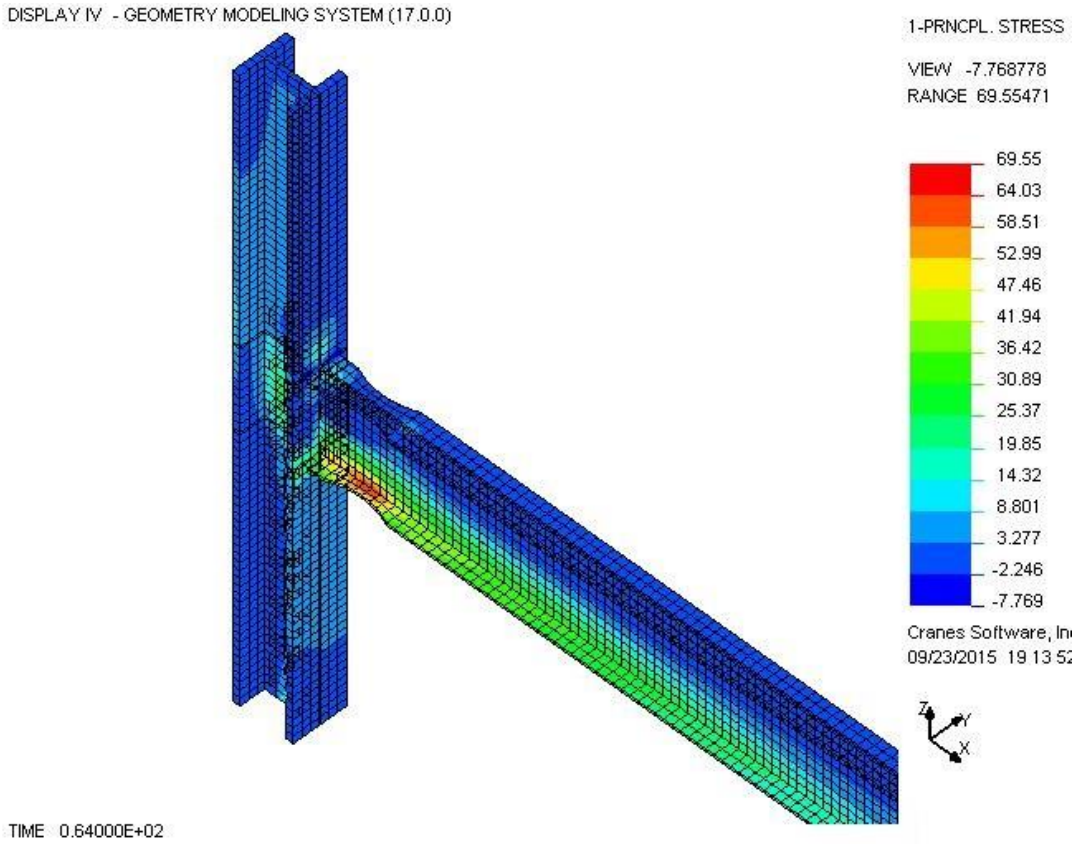

Figure 4.2.1:1st Principal stress (model 1a)

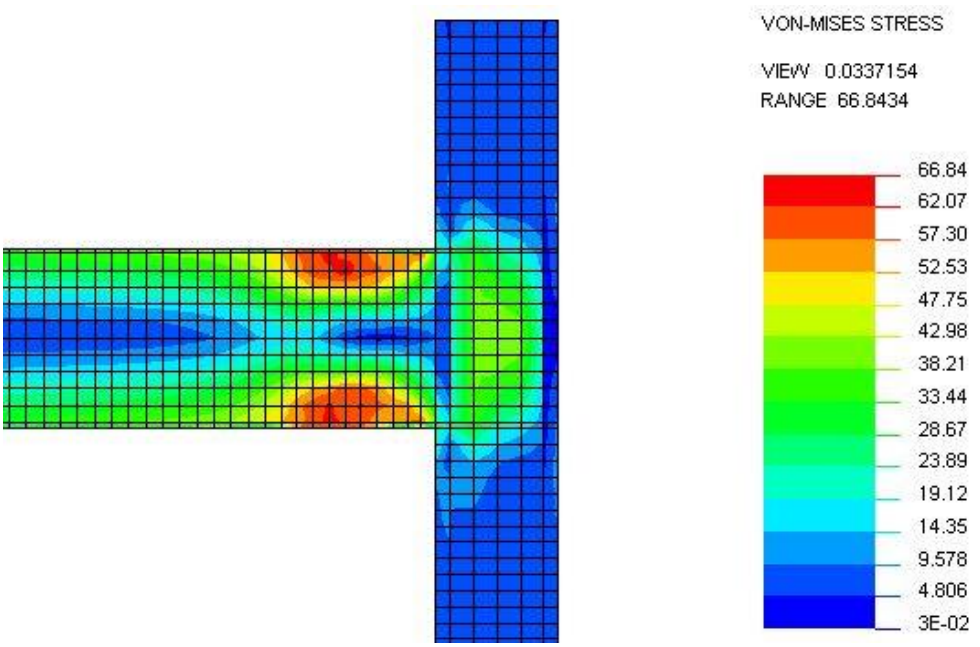

Figure 4.2.2: Enlarged view of Plastic Hinge entering the beam web (Model 1a)

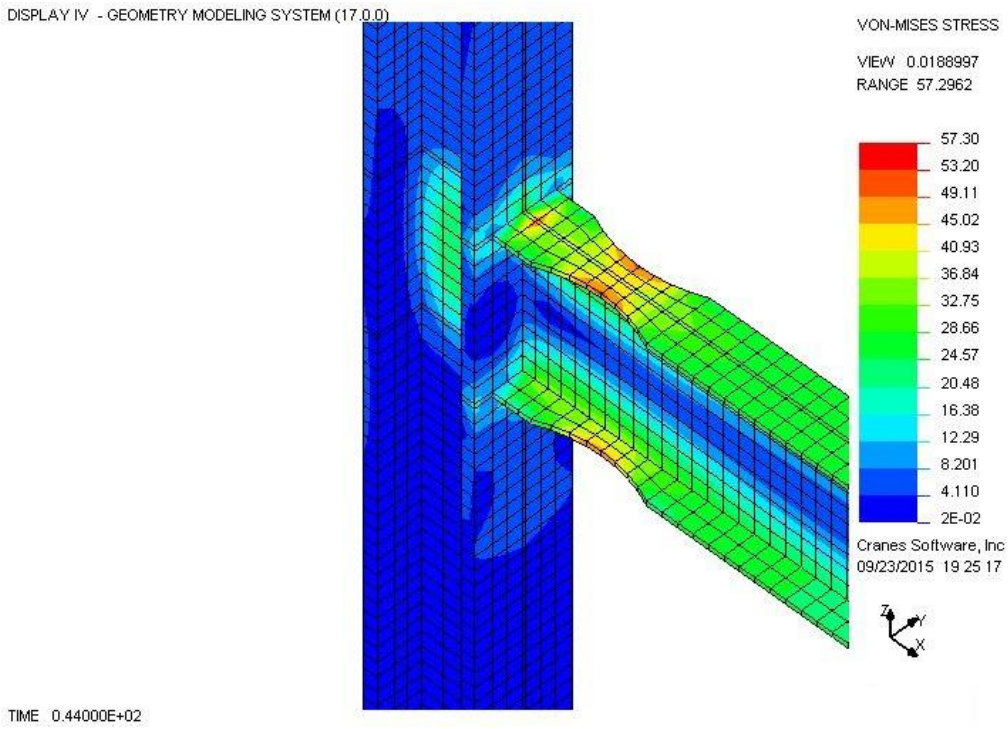

Figure 4.2.3: Von-Mises Stress distribution at yield point (Model 1a)

In the model 2a, as shown in Figure 4.2.4 and Figure 4.2.5, 1st Principal stress reached 71.23 ksi and Von-Mises stress reached 68.26 ksi respectively at time step 70 (The last step at which the 1st Principal stress is less than 84 ksi). Figure 4.2.5 shows that the yielding Von-Mises stress has entered the web causing plastic hinge in the reduced section which is the desired result. Similarly, Figure 4.2.6 represents the Von-Mises stress reaching yield value of 57.72 ksi at time step 42.

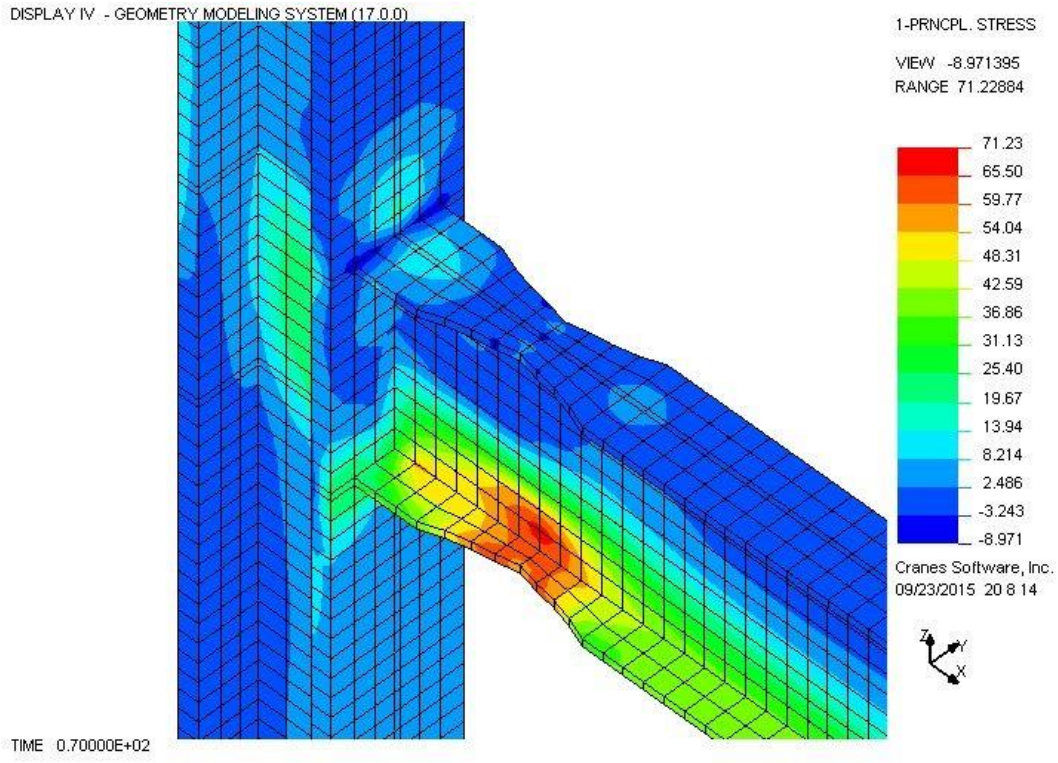

Figure 4.2.4:1st Principal stress (model 2a)

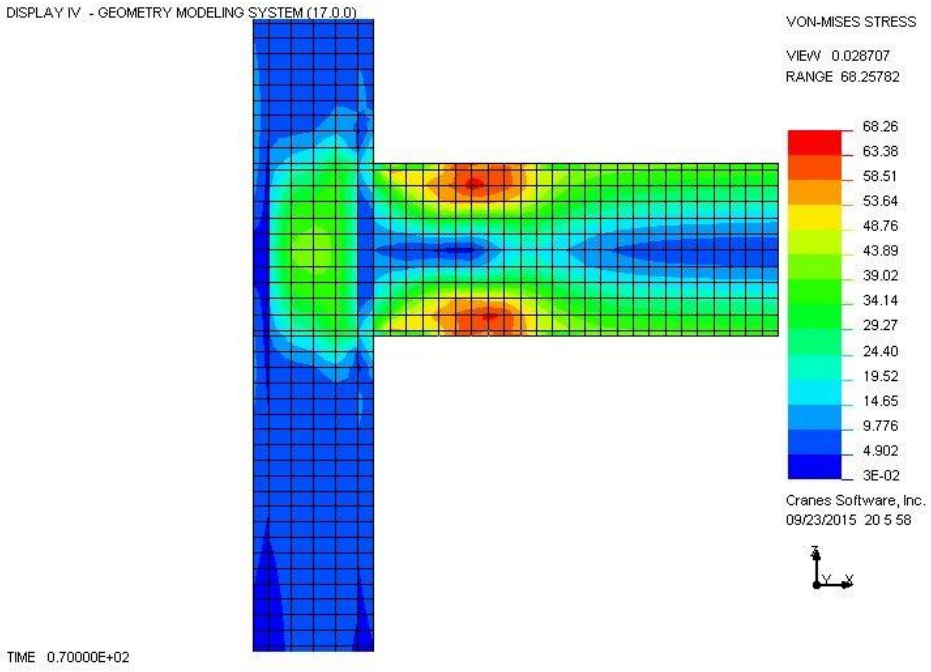

Figure 4.2.5: Enlarged view of Plastic Hinge entering the beam web (Model 2a)

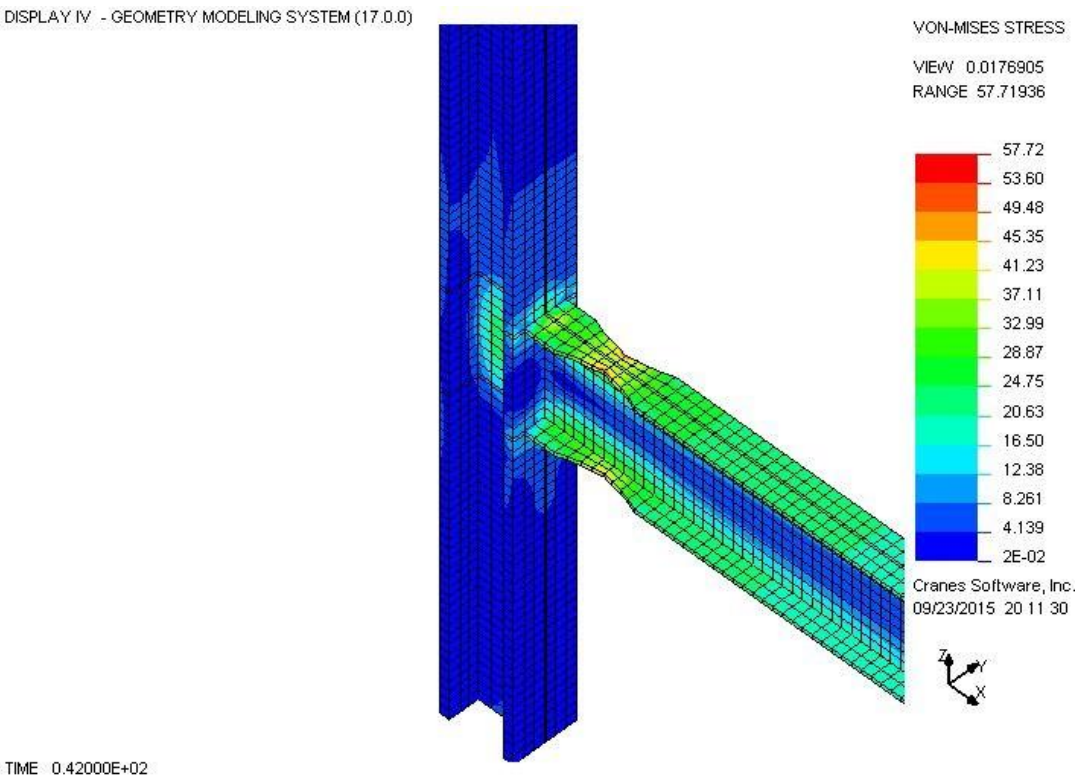

Figure 4.2.6: Von-Mises Stress distribution at yield point (Model 2a)

4.3 Composite slab frame

In the model 1b, as shown in Figure 4.3.1 and Figure 4.3.2, 1st Principal stress reached 74.45 ksi and Von-Mises stress reached 72.56 ksi respectively at time step 87 (The last step at which the 1st Principal stress is less than 84 ksi). Figure 4.3.2 shows that, the yielding Von-Mises stress has entered the web causing plastic hinge in the reduced section which is the desired result. Similarly, Figure 4.3.3 represents the Von-Mises stress reaching yield value of 57.25 ksi at time step 53.

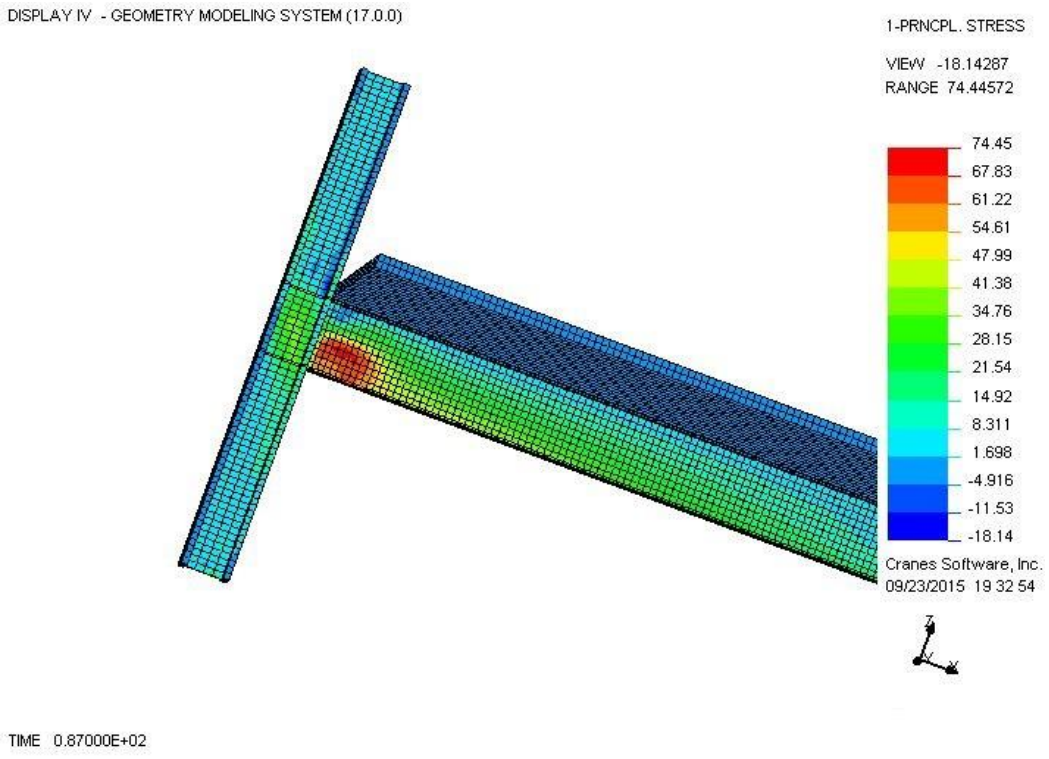

Figure 4.3.1:1st Principal stress (model 1b)

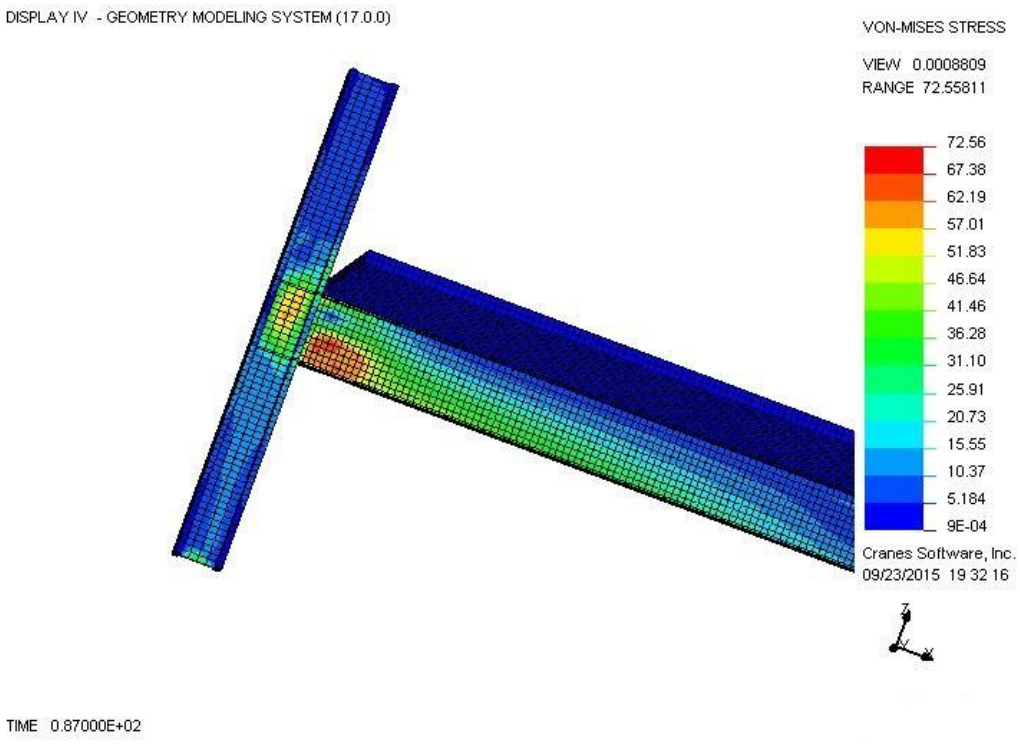

Figure 4.3.2: Enlarged view of Plastic Hinge entering the beam web (Model 1b)

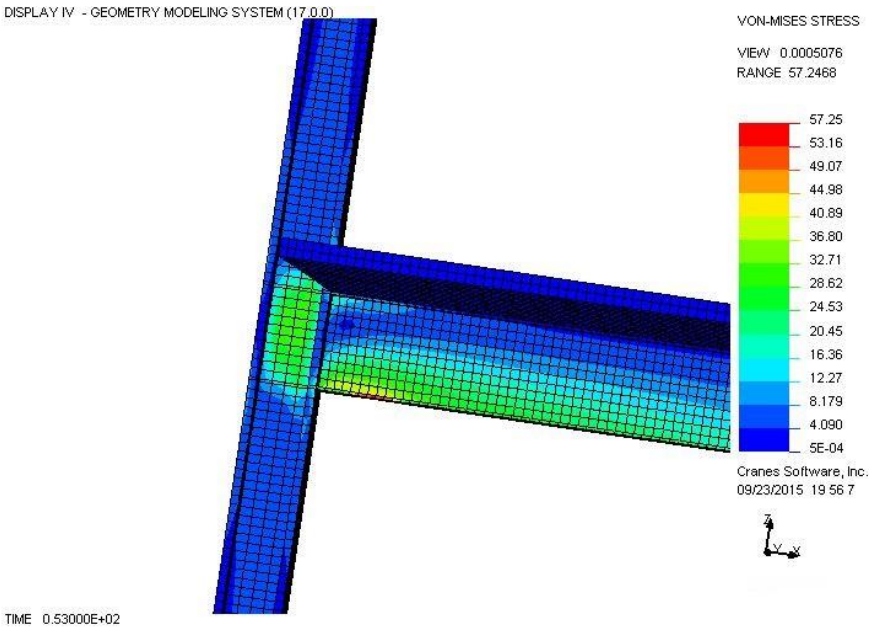

Figure 4.3.3: Von-Mises Stress distribution at yield point (Model 1b)

In the model 2b, as shown in Figure 4.3.4 and Figure 4.3.5, 1st Principal stress reached 81.16 ksi and Von-Mises stress reached 79.77 ksi respectively at time step 94 (The last step at which the 1st Principal stress is less than 84 ksi). Figure 4.3.5 shows that the yielding Von-Mises stress has entered the web causing plastic hinge in the reduced section which is the desired result. Similarly, Figure 4.3.6 represents the Von-Mises stress reaching yield value of 57.75 ksi at time step 51.

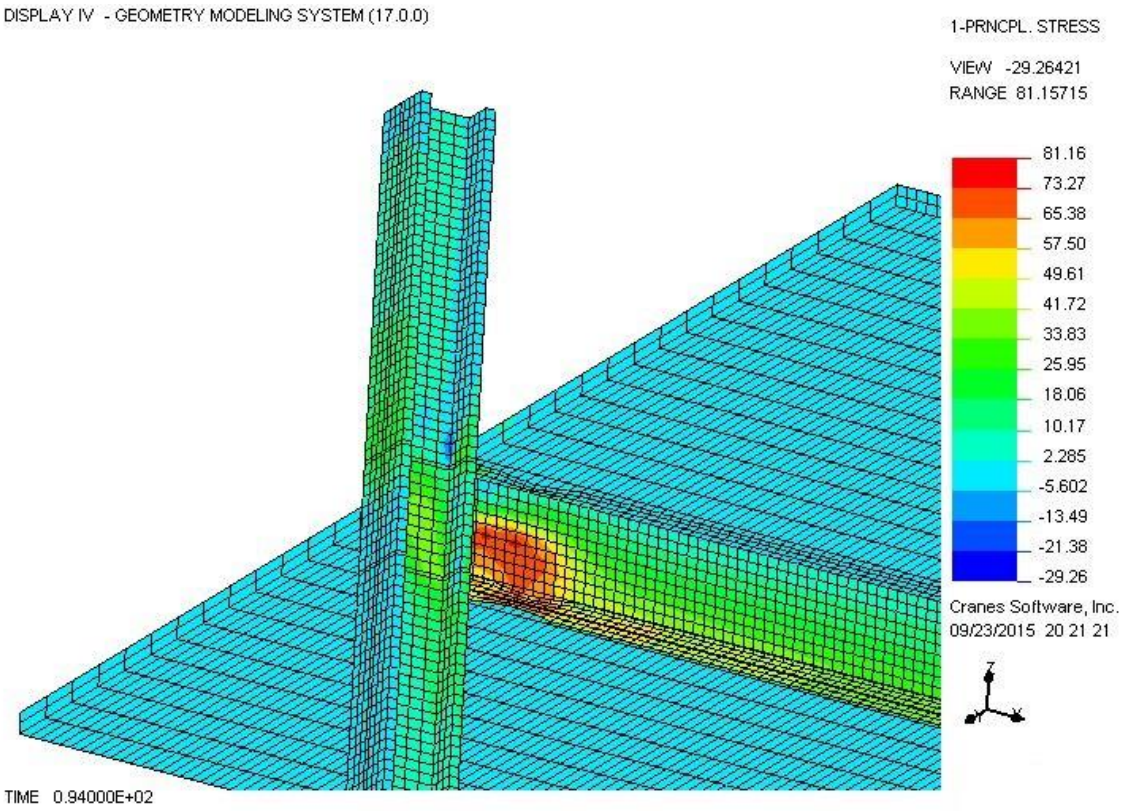

Figure 4.3.4:1st Principal stress (model 2b)

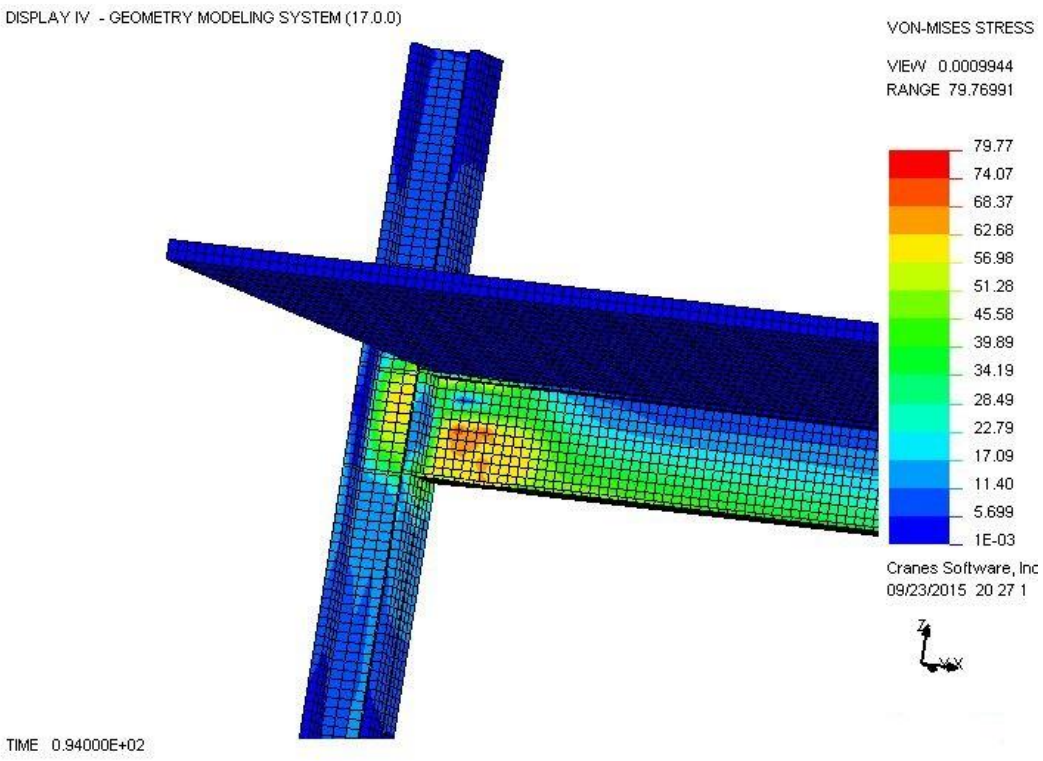

Figure 4.3.5: Enlarged view of Plastic Hinge entering the beam web (Model 2b)

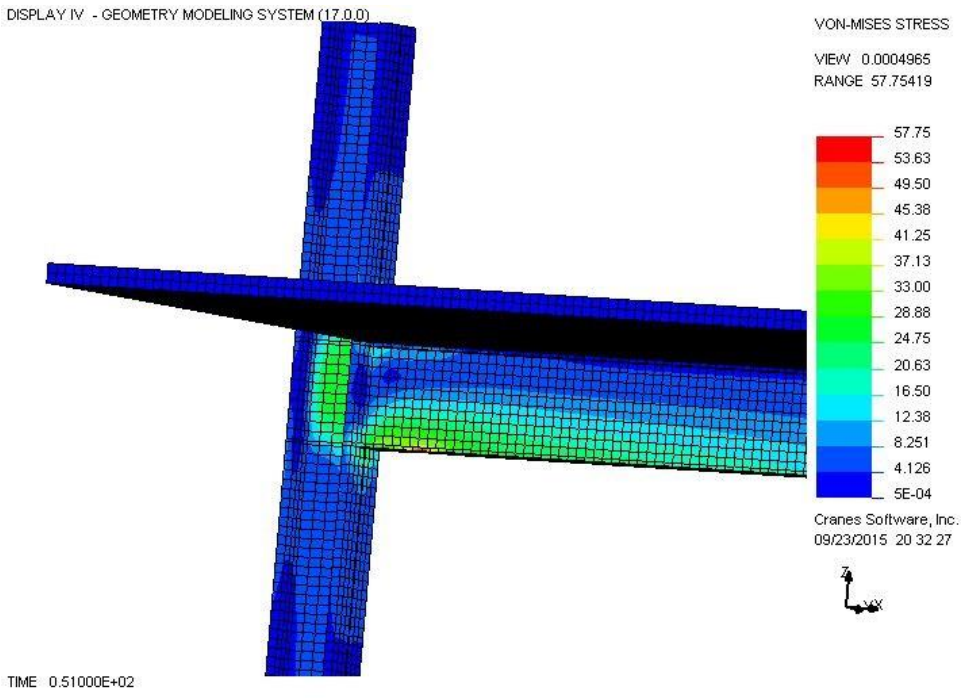

Figure 4.3.6: Von-Mises Stress distribution at yield point (Model 2b)

4.4 Ductility

Ductility refers to the elongation in a material caused after the material has yielded or crossed elastic limit. It is the measure of strain the material can take before fracture. The ductility of the frame is calculated as:

Ductility = Frame lateral movement at fracture point/ Frame lateral movement at yield point

The Figure 4.4.1 below shows the lateral movement (Δ) of a typical frame.

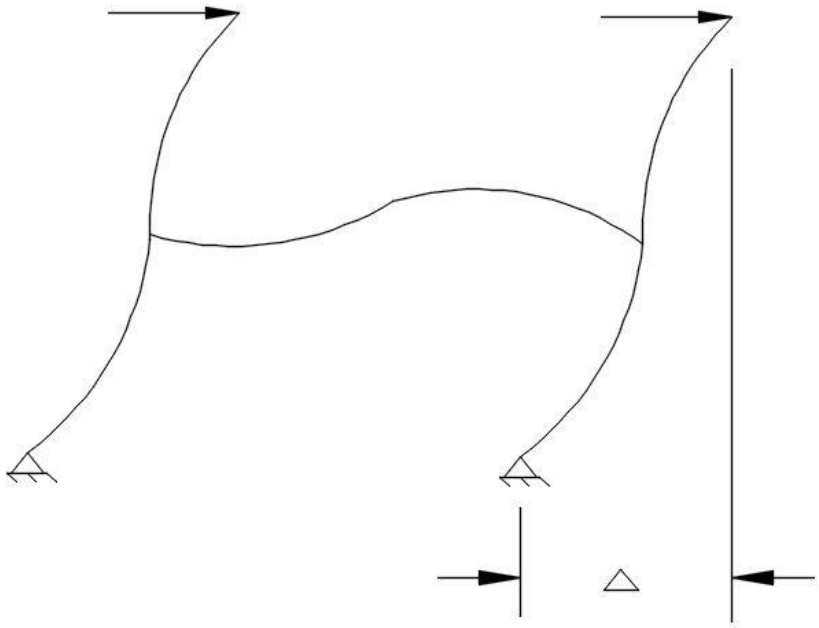

Figure 4.4.1: lateral movement (Δ) of a frame

Table 4.4-1: Lateral movement of frames at yield and fracture points

Model	Frame lateral movement at yield point (Δ_y) (in)	Frame lateral movement at fracture point (Δ_u) (in)
Bare Steel Frame (Model 1a)	1.46	2.34
Composite Slab Frame (Model 1b)	1.32	3.29
Bare Steel Frame (Model 2a)	1.32	2.52
Composite Slab Frame (Model 2b)	1.21	4.06

Table 4.4-2: Ductility comparison of frames

Model	Ductility ($=\Delta_u/\Delta_y$)
Bare Steel Frame (Model 1a)	2.34/1.46 = 1.60
Composite Slab Frame (Model 1b)	3.29/1.32 = 2.49
Bare Steel Frame (Model 2a)	2.52/1.32 = 1.91
Composite Slab Frame (Model 2b)	4.06/1.21 = 3.35

It is seen from the non-linear analysis that the ductility of frames with composite slab is larger than the bare steel frames. The ductility ratio of the two frames can be determined as:
Ductility ratio = ductility of frame with composite slab/ ductility of frame with bare steel

For model 1,

Ductility ratio = 2.49/1.60

= 1.55

For model 2,

Ductility ratio = 3.35/1.91

= 1.75

From the ductility comparison, the ductility of frame with a composite slab is 55 % more than that of the bare steel frame for model 1 and 75 % more than that of bare steel frame for model 2. More models could be analyzed so that a range of percentage increase in ductility can be suggested.

4.5 Strength

The strength ratio of the frame can be determined as:

Strength ratio= time step for model with a composite slab/ time step for model with bare steel.

For comparing the strength, the time step is noted for each model at fracture. The model with higher time step for same lateral load and same boundary conditions is stated to be the stronger one.

Table 4.5-1: Strength comparison of frames

Model	Time step until fracture	Strength ratio
Bare Steel Frame (Model 1a)	64	87/64 = 1.36
Composite Slab Frame (Model 1b)	87	
Bare Steel Frame (Model 2a)	70	94/70 = 1.34
Composite Slab Frame (Model 2b)	94	

It is seen that the strength of frame with a composite slab is 36 % more than that of the bare steel frame for Model 1 and 34 % more than that of the bare steel frame for Model 2. It can be seen that the composite slab frames are able to take more load than the bare steel frames which can be due to the composite effect of the slab on the frames. A range of percentage increase in the strength can be suggested by performing analyses for more models.

4.6 Stiffness

Stiffness is defined as the rigidity of the object due to which it resists the deformation under the applied load. The stiffness is calculated as:

Stiffness = Applied lateral load/Lateral displacement of the column

Since the stiffness is calculated within the elastic range, the Von-Mises stress produced by the lateral load should be less than 57 ksi. The maximum value of Von-Mises is 57 ksi before yielding occurs. An arbitrary lateral load of 20 kips (Since, the maximum Von-Mises stress due to 20 kips is less than 57 ksi) is applied on all the frames to observe the deflection which is used in the calculation the stiffness of frames.

Table 4.6-1: Lateral displacement of frames within elastic range

Model Type	Lateral load (P) (kips)	Max Deflection (Δ) (in)
Bare Steel Frame (Model 1a)	20	0.889
Composite Slab Frame (Model 1b)	20	0.653
Bare Steel Frame (Model 2a)	20	0.788
Composite Slab Frame (Model 2b)	20	0.584

Table 4.6-2: Stiffness ratio calculation and comparison between frames

Model Type	Stiffness ratio (=P/Δ) (kips/in)
Bare Steel Frame (Model 1a)	=20/0.889 = 22.497
Composite Slab Frame (Model 1b)	=20/0.653 = 30.627
Bare Steel Frame (Model 2a)	=20/0.788 = 25.381
Composite Slab Frame (Model 2b)	= 20/0.584 = 34.246

It is seen that the stiffness ratio of composite slab frames is greater than that bare steel frames. The stiffness ratio of composite slab frame with respect to bare steel frame is determined as:

Stiffness ratio =Lateral movement of bare steel frame/Lateral movement of composite slab frame

For Model 1,

Stiffness ratio = 30.627/22.497

= 1.36

For Model 2,

Stiffness ratio = 34.246/25.381

= 1.35

The calculation shows that the composite slab frame is about 36 % stiffer than the bare steel frame for Model 1 and 35 % stiffer for Model 2. A range of percentage increase in stiffness can be suggested by performing analyses of more models.

CHAPTER 5

CONCLUSION

It is not possible to make buildings invulnerable to earthquake forces. The basic intent of building design technique is to provide buildings with an ability to withstand intense ground shaking without collapse but with some potential structural damage. The objective of building design is to make a building as ductile as possible so that it can withstand large inelastic deformation without the development of instability and collapse.

Since the Northridge Earthquake caused brittle failures of steel moment frames which were once called the most ductile connection system, a lot of analytical and experimental research has been carried out to study the effect of various connection elements in the performance of the frame as a whole.

The purpose of this research was to study the effect of a composite slab on the ductility, strength and stiffness of the steel moment frames with Reduced Beam Sections. A finite element analysis software, NISA DISPLAY IV, was used to model and analyze the frame. From the analyzed model, the Von-Mises Stress, the 1st Principal Stress, and lateral movements of frames were observed and comparison was done between frame with bare steel and with composite slab based on their ductility, strength and stiffness.

From the observation, the composite slab frame had more ductility, strength and stiffness than the bare steel frame. The results of the analyses can be summarized as: a) the ductility of the composite slab frame is 55 % more than that of the bare steel frame in model 1 and 75 % more in model 2, b) the strength of the composite slab frame is 36 % more than that of the bare steel frame in model 1 and 34 % more in model 2, and c) the stiffness of the composite slab frame is

36 % more than that of the bare steel frame in model 1 and 35 % more in model 2. However, more model analyses could be conducted to suggest a range of percentage increase.

The results were compatible with most of the research done which stated that the composite slabs have a stabilizing effect on the RBS moment connections increasing the load carrying capacity of the frames. The presence of slabs proved to be beneficial by enhancing beam stability and delaying strength degradation.

REFERENCES

American Institute of Steel Construction (AISC). (2012). *Steel Construction Manual.14th Ed*., Chicago, IL.

American Institute of Steel Construction (AISC). (2012). *Seismic Design Manual, 2nd Ed*., Chicago, IL.

Bartlett, F.M., Dexter, R.J., Graeser, M.D., Jelinek, J.J, Schmidt, B.J., and Galambos, T.V. (2001) "Updating Standard Shape Material Properties Database for Design and Reliability."AISC Research Project #99001, Chicago, IL American Institute of Steel Construction.

Chen, S.-J., Tsao, Y., & Chao, Y. (2001). "Enhancement of ductility of existing seismic steel moment connections." Journal of Structural Engineering, 127(5), 538-545.

Civjan, S. A., Engelhardt, M. D., & Gross, J. L. (2000). "Retrofit of pre-Northridge moment-resisting connections." Journal of Structural Engineering, 126(4), 445-452.

Civjan, S. A., Engelhardt, M. D., & Gross, J. L. (2001). "Slab effects in SMRF retrofit connection tests." Journal of Structural Engineering, 127(3), 230-237.

Engelhardt, M. D., Winneberger, T., Zekany, A. J., & Potyraj, T. J. (1996). "The dogbone connection: Part II." Modern Steel Construction, 36(8), 46-55.

Englehardt, M., Winneberger, T., Zekany, A., & Potyraj, T. (1997). "Experimental investigation of dogbone moment connections." American Institute of Steel Construction, Inc.(USA),12.

FEMA-350. (2000). 350—*Recommended seismic design criteria for new steel moment-frame buildings*. Washington (DC): Federal Emergency Management Agency.

Hamburger, R. O., Krawinkler, H., Malley, J. O., & Adan, S. M. (2009). "Seismic design of steel special moment frames: a guide for practicing engineers." National Earthquake Hazards Reduction Program.

Han, S.-W., Moon, K.-H., & Stojadinovic, B. (2009). "Design equations for moment strength of RBS-B connections." Journal of Constructional Steel Research, 65(5), 1087-1095.

Hedayat, A. A., & Celikag, M. (2009)."Post-Northridge connection with modified beam end configuration to enhance strength and ductility." Journal of Constructional Steel Research, 65(7), 1413-1430.

Iwankiw, N. (2004). "Seismic design enhancements and the reduced beam section detail for steel moment frames." Practice Periodical on Structural Design and Construction, 9(2), 87-92.

Jin, J., & El-Tawil, S. (2005). "Seismic performance of steel frames with reduced beam section connections." Journal of Constructional Steel Research, 61(4), 453-471.

Jones, S. L., Fry, G. T., & Engelhardt, M. D. (2002). "Experimental evaluation of cyclically loaded reduced beam section moment connections." Journal of Structural Engineering, 128(4), 441-451.

Lee, C.-H., & Chung, S. W. (2007). "A simplified analytical story drift evaluation of steel moment frames with radius-cut reduced beam section." Journal of Constructional Steel Research, 63(4), 564-570.

Moore, K. S., Malley, J. O., & Engelhardt, M. D. (1999). "Design of reduced beam section (RBS) moment frame connections." Steel Committee of California.

NISA/DISPLAY IV Ver. 17.0 (Finite Element Software). (2010). Engineering Mechanics Research Corporation, Troy, MI.

Park, J. W., & Hwang, I. (2003). “Experimental investigation of reduced beam section connections by use of web openings.” Engineering Journal, 40(2), 77-88.

Roeder, C. W. (2002a). “Connection performance for seismic design of steel moment frames.” Journal of Structural Engineering, 128(4), 517-525.

Roeder, C. W. (2002b). “General issues influencing connection performance.” Journal of Structural Engineering, 128(4), 420-428.

Sophianopoulos, D., & Deri, A. (2011). “Parameters affecting response and design of steel moment frame reduced beam section connections: an overview.” International Journal of Steel Structures, 11(2), 133-144.

Spacone, E., & El-Tawil, S. (2004). “Nonlinear analysis of steel-concrete composite structures: State of the art.” Journal of Structural Engineering, 130(2), 159-168.

Wang, C. K., Salmon, C.G., and Pincheira, J.A. (2007). *Reinforced concrete design.* 7th ed., John Wiley & Sons, Hoboken, NJ.

Zhang, X., & Ricles, J. M. (2006). “Experimental evaluation of reduced beam section connections to deep columns.” Journal of Structural Engineering, 132(3), 346-357.

APPENDICES

APPENDIX.A

RBS CONNECTION DESIGN CALCULATIONS

(AISC SEISMIC DESIGN MANUAL, Using Examples 4.3.4)

MODEL 1

Beam Property (W 21 ×62)	Column Property (W 12 ×190)
b_f= 8.24 in.	b_f =12.7 in.
d_b= 21 in.	d_c =14.4 in.
t_f = 0.615 in.	t_f =1.74 in.
t_w = 0.4 in.	t_w = 1.06 in.
Z_x = 144 in^3	Z_x= 311 in^3
I_x = 1330 in^4	I_x = 1890 in^4
A_b = 18.3 in^2	A_c = 56 in^2

Check beam requirement *(Seismic design manual page 4-58)*

The W 21×62 beam satisfy the requirement of ANSI/ASCI 352 Section 5.3.1 as a rolled wide flange member, with depth less than a W 36, weight less than 300 lb/ft and flange thickness less than 1.75. The clear span to depth ratio of the beam is at least 7 as required for an SMF system:

Clear span/depth = (span length – d_c)

Where,

d_b = beam depth

d_c = depth of column

Clear span/depth = (30×12 – 14.4)/21

= 16.457 ≥ 7 (O.K.)

Check column requirement **(***Seismic design manual page 4-59)*

The W 12×190 satisfies the requirement of section the requirement of section 5.3.2 as a rolled wide flange member, with the frame beam connected to the column flange and with a column depth less than a W 36.

ANSI/ASIC 358 Section 5.8: *(AISC Seismic design manual page 4-59, 4-60)*

Step 1: Trial dimension of RBS

$a \approx (0.5 \text{ to } 0.75) \times b_f$

Where, b_f= width of beam flange

$0.5\times b_f \leq a \leq 0.75\times b_f$

$4.12 \text{ in} \leq a \leq 6.18 \text{ in}$

Take a = 5 in.

$b \approx (0.65 \text{ to } 0.85) \times d_b$

Where, d_b= depth of beam

$0.65\times d_b \leq b \leq 0.85\times d_b$

$13.65 \text{ in} \leq b \leq 17.85 \text{ in}$

Take b = 15 in.

$c \approx (0.1 \text{ to } 0.25)\times b_f$

$0.1\times b_f \leq c \leq 0.25\times b_f$

$0.824 \leq c \leq 2.06$

Take c = 1.65in

Step 2: Plastic Section Modulus at the center of the reduced beam *(AISC seismic design manual*

page 4-53 and 4-60)

$Z_{RBS} = Z_X - 2 \times c \times t_{bf} \times (d_b - t_{bf})$

$= 144 - 2 \times 1.65 \times 0.615 \times (21 - 0.615)$

$= 102.628 \text{ in}^3$

Step 3: Probable Maximum Moment at the center of RBS: *(AISC seismic design manual Page 4-60, 4-61)*

$C_{pr} = \left(\frac{F_y + F_y}{2 \times F_y}\right) = \left(\frac{50+65}{2 \times 50}\right) = 1.15$ (For A992 Steel)

Where,

F_y = The specified minimum yield stress of the material of the yielding element

= 50 Ksi (For A992 Steel)

F_u = The ultimate tensile stress of the material of the yielding element

= 65 Ksi (For A992 Steel)

C_{pr} = A factor to account for the peak connection strength, including strain hardening, local restraint, additional reinforcement, and other connection connections.

$Mpr = C_{pr} \times R_y \times F_y \times Z_{RBS}$ *(ANSI/ AISC 358 Eq. 5.8-5)*

Where,

Z_{RBS} = Plastic modulus of the section at the location of the plastic hinge

R_y = Ratio of the expected yield strength to the minimum specified yield Steel to be used

= 1.1 *(From AISC seismic provision Table A3.1)*

$M_{pr} = 1.15 \times 1.1 \times 50 \times 102.628$

$= 6491.22$ K-in

Step 4: Shear Force at the center of the reduced beam sections at each end of the beam:

(AISC Seismic design manual page. 4- 61, 4-62)

$W_u = 1.2\ D + 0.5\ L + 0.2\ S$

Where,

D = Dead load

L = Live load

S = Snow load

$W_u = 1.2 \times 0.\ 840 + 0.5 \times 0.600 + 0.2 \times 0$

=1.31 k/ft.

= 0.1 k/in.

Distance from the column face to the center of RBS cut,

$S_h = a + b/2$ *(ANSI/ AISC 358 figure 5.2)*

$= 5 + 15/2$

= 12.5 in.

Distance from the center of the RBS cut to the end of the half beam,

$L_h = L - 2 \times (d_c/2) - 2 \times S_h$

$= 30 \times 12$ in. $- 2 \times (14.4$ in. $/2) - 2 \times 12.5$ in.

= 320.6 in.

$V_{RBS} = 2 \times M_{RBS} / L_h + w_u \times L_h /2$ *(AISC Seismic design manual page. 4- 62, Fig 5-12)*

$= (2 \times 6491.22$ k-in$)/ 320.6$ in $+ (0.1$ k/in $\times 320.6$ in$)/ 2$

= 56.524 kips

$V'_{RBS} = 2 \times M_{RBS} / L_h - w_u \times L_h /2$

$= (2 \times 6491.22$ k-in$)/ 320.6$ in $- (0.1$ k/in $\times 320.6$ in$)/ 2$

= 24.464 kips

Step 5: Probable Maximum Moment at the face of the column: *(AISC Seismic design manual page. 4-63, 4- 64)*

$M_f = M_{pr} + V_{RBS} \times S_h$ *(ANSI/ AISC 358 Eq. 5.8-6)*

(Fig 5-12 AISC Seismic design manual)

M_{pr} = Probable Maximum Moment at the center of RBS

V_{RBS} = Shear at the center of reduced beam section

M_f = 6491.22 k-in + 56.524 kips × 12.5 in

= 7197.77 k-in

$M'_f = M_{pr} + V'_{RBS} \times S_h$

= 6491.22 k-in – 24.464 kips × 12.5in

= 6185.42 k-in

Step 6: Plastic moment of the beam based on the expected yield stress: *(AISC Seismic manual page. 4-64)*

$M_{pe} = R_y \times F_y \times Z_x$ *(ANSI/ AISC 358 Eq. 5.8-7)*

M_{pe} =1.1 × 50 k/in^2 × 144 in^3

= 7920 k – in

Alternatively, using ASIC Seismic Manual Table 4-2 for W 21 x 62 beam,

R_yM_p = 660 k-ft. = 7920 k-in

Step 7: Check Mf moment at the face of column should not exceed $\phi_d M_{pe}$: *(AISC Seismic design manual page. 4-65)*

From ANSI/ AISC 358 section 2.4.1

ϕ_d = 1.0 0

$\phi_d M_{pe}$ = 1.00 × 7920

= 7920 k-in.

$M_f \leq \phi_d M_{pe}$ *(ANSI/ AISC 358 Eq. 5.8-8)*

M_f = 7197.77 k-in. $\leq \phi_d M_{pe}$ = 7920 k-in. (OK.)

Thus, the preliminary dimensions of RBS are OK.

Step 8: Required Shear Strength, Vu, of the beam and beam web-to-column connection,

(AISC Seismic design manual page 4-61, 4-62)

$V_u = V_{RBS} + w_u \times S_h$

V_{RBS} = Shear at the center of reduced beam section

W_u = uniformly distributed load on beam

$V_u = 56.524 + (1.31/ 12 \times 12.5)$

= 57.888 kips

Note that there is little error in taking $V_u = V_{RBS.}$

Step 9: Design the beam web to column connection according to ANSI/ASCI 358 Section 5.6:

(AISC Seismic design manual page. 4-65, 4-66)

AISC specification section G2.1

$d_{min} = V_u / \phi \times 0.6 \times F_y \times t_w \times C_v$,

$C_v = 1.0$ *(AISC specification section G2.1)*

$d_{min} = 57.888 / (1.0 \times 0.6 \times 50 \times 0.4 \times 1.0)$

= 4.824 in.

By inspection sufficient depth remains.

Step 10: Continuity plate requirements according to ANSI/AISC 358 Chapter 2:

(AISC Seismic design manual page. 4-66)

t_{cf} = 1.74 in

$R_{yb} = R_{yc} = 1.1$ *(AISC seismic provision Table A3.1)*

$$t_{cf} \geq 0.4 \times \sqrt{1.8 \times b_{bf} \times t_{bf} \times \frac{Ryb \times Fyb}{Ryc \times Fyc}}$$ *(Provision equation E3-8)*

Where,

t_{cf} = The minimum required thickness of column flange when no continuity plates are provided, inches

b_{bf} = The width of the beam flange, inches

t_{bf} = Thickness of the beam flange, inches

$F_{yb} = F_{yc}$ = Specified minimum yield stress of the beam or column flange, ksi

$R_{yb} = R_{yc}$ = ratio of the expected yield strength of the beam (column) material to the minimum specified yield strength

=1.1, for the ASTM A992 steel beam or column, respectively

$$t_{cf} \geq 0.4 \times \sqrt{1.8 \times 8.24 \times 0.615 \times \frac{1.1 \times 50}{1.1 \times 50}}$$

$1.74 \geq 1.208$ in

OR

$$t_{cf} \geq \frac{b_{bf}}{6}$$ *(Provision equation E3-9)*

$$1.74 \geq \frac{8.24}{6}$$

$1.74 \geq 1.37$

Therefore, from both the provisions it is seen that continuity plates are not required.

Step 11: Check beam column beam relationship per ANSI/AISC Section 5.4:

(AISC Seismic design manual page. 4-69, 4-70)

$\frac{\sum M_{pc}^{*}}{\sum M_{pb}^{*}} > 1.0$ *(Provision Eq. E3-1)*

$$\sum M_{pc}{}^{*} = Z_{xt} \times \left[F_y - \frac{P_{uc}}{A_g}\right]\left[\frac{h_t}{h_t - \frac{d_b}{2}}\right] + Z_{xb} \times \left[F_y - \frac{P_{uc}}{A_g}\right]\left[\frac{h_b}{h_b - \frac{d_b}{2}}\right]$$

P_{uc} = 249 kips *(ASIC Seismic Design Example 4.3.2, page. 70)*

$$\sum M_{pc}{}^{*} = 311 \times \left[50 - \frac{249}{55.8}\right]\left[\frac{75}{78 - \frac{21}{2}}\right] + 311 \times \left[50 - \frac{249}{55.8}\right]\left[\frac{75}{78 - \frac{21}{2}}\right]$$

= 32935.35 kip- in

The expected flexural demand of the beam at the column centerline is defined in ANSI/AISC 358 Section 5.4 as:

$\sum M_{pb}{}^{*} = \sum(M_{pr} + M_{uv})$ *(ANSI/ AISC 358 section 5.4)*

$\sum M_{uv} = (V_{RBS} + V'_{RBS})\left(a + \frac{b}{2} + \frac{d_c}{2}\right)$

= (56.524 kips + 24.464 kips) $\left(5 \text{ in} + \frac{15}{2}\text{in} + \frac{14.4}{2}\text{in}\right)$

= 1595.46 kip-in

Therefore expected flexural demand of the beam at the column center line is:

$\sum M_{pb}{}^{*} = 2 \times M_{pr} + \sum M_{uv}$

= 2 × (6491.22) + 1595.46

= 14577.9 kip-in

$\frac{\sum M_{pc}^{*}}{\sum M_{pb}^{*}} = \frac{32935.35}{14577.9}$ *(AISC Seismic design manual page. 4-71)*

= 2.259 > 1.0 (O.K.)

Therefore, strong-column-weak-beam check is satisfied.

Perform Panel Zone Check

$$V_c = \frac{M_f + M_f'}{\left(\frac{h_t}{2} + \frac{h_b}{2}\right)}$$

$$= \frac{7199.77 + 6185.42}{\left(\frac{75}{2} + \frac{75}{2}\right)}$$

$$= 178.469 \text{ kips}$$

Where,

h_t = Story height above the joint, inches

h_b = Story height below the joint, inches

M_f = Moment at the face of the column, kip-inches

The required strength of the panel zone is:

$$R_u = \frac{\sum M_f}{(d_b + t_f)} - V_c$$

$$= \frac{7197.77 + 6185.42}{(21 - 0.615)} - 178.469$$

$$= 478.06 \text{ kips}$$

Where,

V_c = Shear in column due to plastic hinging of the RBS

t_f = Thickness of beam flange

d_b = Depth of the beam

P_r = 243 kips *(AISC Seismic design manual Example 4.3.2, page. 4-72)*

$P_r < 0.75\ P_c$

$P_r < 0.75 \times F_y \times A_g$

$< 0.75 \times 50 \times 56$

P_r = 243 kips < 2100 kips (O.K.)

Shear strength of the panel zone is given by AISC specification equation J 10-11:

$$\phi R_n = \phi \times 0.6 \times F_y \times d_c \times t_w \times \left[1 + \frac{3 \times b_{cf} \times t_{cf}^2}{d_b \times d_c \times t_w}\right]$$

$$= 1.00 \times 0.60 \times 50 \times 14.4 \times 1.06 \times \left[1 + \frac{3 \times 12.7 \times 1.74^2}{21 \times 14.4 \times 1.06}\right]$$

$$= 622.71 \text{ kips}$$

Where,

d_b = Depth of beam, inches

d_c = Depth of column, inches

t_w = Web thickness of column, inches

t_{cf} = Flange thickness of column, inches

b_{cf} = Width of the column, inches

ϕ = 1.00

Alternatively, using Table 4-2 of AISC Seismic Design Manual for W 12×190:

$0.75 \times P_y$ = 2100 kips

ϕR_{v1} = 458 kips

ϕR_{v2} = 3460 kip-in

$\phi R_n = R_{v1} + \phi R_{v2}$

$$= 458 + \frac{3460}{21}$$

$$= 622.76 \text{ kips}$$

Since, R_u = 478.06 kips < ϕR_n = 622.76 kips, a column-web doubler plates are not required.

Lateral load calculation for bare steel frame:

From the calculation, the moment on each column face is, M_f = 7197.77 k-in

$$= \frac{7197.77}{12} \text{ k-ft} = 599.81 \text{ k-ft}$$

Since, the moment developed on the beam column connection is caused by the column below and above the connection; moment about each column is given as,

$$\frac{M_f}{2} = 299.91 \text{ k-ft}$$

The height of the column above the beam column connection is 6ft and 3 inches.

So, the lateral load is calculated to be:

$$\frac{299.91 \text{ k}-\text{ft}}{6.25 \text{ ft}} = 47.98 \text{ kips}$$

MODEL 2

Beam Property (W 21 ×73)	Column Property (W 12 ×210)
b_f= 8.30 in.	b_f =12.8 in.
d_b= 21.2 in.	d_c =14.7 in.
t_f = 0.740 in.	t_f =1.90 in.
t_w = 0.455 in.	t_w = 1.18 in.
Z_x = 172 in^3	Z_x= 348 in^3
I_x = 1600 in^4	I_x = 2140 in^4
A_b = 21.5 in^2	A_c = 61.8 in^2

Check beam requirement *(Seismic design manual page 4-58)*

The W 21×73 beam satisfy the requirement of ANSI/ASCI 352 Section 5.3.1 as a rolled wide flange member, with depth less than a W 36, weight less than 300 lb/ft and flange thickness less than 1.75. The clear span to depth ratio of the beam is at least 7 as required for an SMF system:

Clear span/depth = (span length – d_c)

Where,

d_b = beam depth

d_c = depth of column

Clear span/depth = $(30\times12 - 14.7)/21.2$

$= 16.287 \geq 7$ (O.K.)

Check column requirement (*Seismic design manual page 4-59)*

The W 12×210 satisfies the requirement of section the requirement of section 5.3.2 as a rolled wide flange member, with the frame beam connected to the column flange and with a column depth less than a W 36.

ANSI/ASIC 358 Section 5.8: *(AISC Seismic design manual page 4-59, 4-60)*

Step 1: Trial dimension of RBS

$a \approx (0.5 \text{ to } 0.75) \times b_f$

Where, b_f= width of beam flange

$0.5\times b_f \leq a \leq 0.75\times b_f$

$4.15 \text{ in} \leq a \leq 6.225 \text{ in}$

Take a = 6 in.

$b \approx (0.65 \text{ to } 0.85) \times d_b$

Where, d_b= depth of beam

$0.65\times d_b \leq b \leq 0.85\times d_b$

$13.78 \text{ in} \leq b \leq 18.02 \text{ in}$

Take b = 16 in.

$c \approx (0.1 \text{ to } 0.25)\times b_f$

$0.1\times b_f \leq c \leq 0.25\times b_f$

$0.83\leq c \leq 2.075$

Take c = 1.66in

Step 2: Plastic Section Modulus at the center of the reduced beam *(AISC seismic design manual page 4-53 and 4-60)*

$Z_{RBS}= Z_X - 2\times c \times t_{bf}\times (d_b - t_{bf})$

$= 172 - 2\times 1.66\times 0.740\times (21.2 - 0.740)$

$= 121.734\ in^3$

Step 3: Probable Maximum Moment at the center of RBS: *(AISC seismic design manual Page 4-60, 4-61)*

$C_{pr}=\left(\frac{F_y+F_y}{2\times F_y}\right) = \left(\frac{50+65}{2\times 50}\right)=1.15$ (For A992 Steel)

Where,

F_y = The specified minimum yield stress of the material of the yielding element

= 50 Ksi (For A992 Steel)

F_u = The ultimate tensile stress of the material of the yielding element

= 65 Ksi (For A992 Steel)

C_{pr} = A factor to account for the peak connection strength, including strain hardening, local restraint, additional reinforcement, and other connection connections.

$Mpr = C_{pr}\times R_y \times F_y \times Z_{RBS}$ *(ANSI/ AISC 358 Eq. 5.8-5)*

Where,

Z_{RBS} = Plastic modulus of the section at the location of the plastic hinge

R_y = Ratio of the expected yield strength to the minimum specified yield strength of the

Steel to be used

= 1.1 *(From AISC seismic provision Table A3.1)*

$M_{pr} = 1.15 \times 1.1 \times 50 \times 121.734$

= 7699.67 K-in

Step 4: Shear Force at the center of the reduced beam sections at each end of the beam:

(AISC Seismic design manual page. 4- 61, 4-62)

$W_u = 1.2\ D + 0.5\ L + 0.2\ S$

Where,

D = Dead load

L = Live load

S = Snow load

$W_u = 1.2 \times 0.\ 840 + 0.5 \times 0.600 + 0.2 \times 0$

=1.31 k/ft.

= 0.1 k/in.

Distance from the column face to the center of RBS cut,

$S_h = a + b/2$ *(ANSI/ AISC 358 figure 5.2)*

$= 5 + 16/2$

= 13 in.

Distance from the center of the RBS cut to the end of the half beam,

$L_h = L - 2 \times (d_c/2) - 2 \times S_h$

$= 30 \times 12$ in. $- 2 \times (14.7$ in. $/2) - 2 \times 13$ in.

= 319.3 in.

$V_{RBS} = 2 \times M_{RBS} / L_h + w_u \times L_h /2$ (*AISC Seismic design manual page. 4- 62, Fig 5-12)*

$= (2 \times 7699.67 \text{ k-in})/ 319.3 \text{ in} + (0.1 \text{ k/in} \times 319.3 \text{ in})/ 2$

$= 64.193$ kips

$V'_{RBS} = 2 \times M_{RBS} / L_h - w_u \times L_h /2$

$= (2 \times 7699.67 \text{ k-in})/ 319.3 \text{ in} - (0.1 \text{ k/in} \times 319.3 \text{ in})/ 2$

$= 32.263$ kips

Step 5: Probable Maximum Moment at the face of the column: *(AISC Seismic design manual page. 4-63, 4- 64)*

$M_f = M_{pr} + V_{RBS} \times S_h$ *(ANSI/ AISC 358 Eq. 5.8-6)*

(Fig 5-12 AISC Seismic design manual)

M_{pr} = Probable Maximum Moment at the center of RBS

V_{RBS} = Shear at the center of reduced beam section

$M_f = 7699.67 \text{ k-in} + 64.193 \text{ kips} \times 13 \text{ in}$

$= 8534.179$ k-in

$M'_f = M_{pr} + V'_{RBS} \times S_h$

$= 7699.67 \text{ k-in} – 32.263 \text{ kips} \times 13 \text{ in}$

$= 7280.251$ k-in

Step 6: Plastic moment of the beam based on the expected yield stress: *(AISC Seismic manual page. 4-64)*

$M_{pe} = R_y \times F_y \times Z_x$ *(ANSI/ AISC 358 Eq. 5.8-7)*

$M_{pe} = 1.1 \times 50 \text{ k/in}^2 \times 172 \text{ in}^3$

$= 9460$ k – in

Alternatively, using ASIC Seismic Manual Table 4-2 for W 21 x 73 beam,

$R_yM_p = 788$ k-ft. $= 9456$ k-in ≈ 9460 k – in

Step 7: Check Mf moment at the face of column should not exceed $\phi_d M_{pe}$: *(AISC Seismic design manual page. 4-65)*

From ANSI/ AISC 358 section 2.4.1

$\phi_d = 1.0\ 0$

$\phi_d M_{pe} = 1.00 \times 9460$

$= 9460$ k-in.

$M_f \leq \phi_d M_{pe}$ *(ANSI/ AISC 358 Eq. 5.8-8)*

$M_f = 8534.179$ k-in. $\leq \phi_d M_{pe} = 9460$ k-in. (OK.)

Thus, the preliminary dimensions of RBS are OK.

Step 8: Required Shear Strength, Vu, of the beam and beam web-to-column connection,

(AISC Seismic design manual page 4-61, 4-62)

$V_u = V_{RBS} + w_u \times S_h$

V_{RBS} = Shear at the center of reduced beam section

W_u = uniformly distributed load on beam

$V_u = 64.193 + (1.31/ 12 \times 13)$

$= 65.612$ kips

Note that there is little error in taking $V_u = V_{RBS}$.

Step 9: Design the beam web to column connection according to ANSI/ASCI 358 Section 5.6:

(AISC Seismic design manual page. 4-65, 4-66)

AISC specification section G2.1

$d_{min} = V_u / \phi \times 0.6 \times F_y \times t_w \times C_v$,

$C_v = 1.0$ *(AISC specification section G2.1)*

$d_{min} = 65.612 / (1.0 \times 0.6 \times 50 \times 0.455 \times 1.0)$

= 4.807 in.

By inspection sufficient depth remains.

Step 10: Continuity plate requirements according to ANSI/AISC 358 Chapter 2:

(AISC Seismic design manual page. 4-66)

t_{cf} = 1.90 in

$R_{yb} = R_{yc} = 1.1$ *(AISC seismic provision Table A3.1)*

$$t_{cf} \geq 0.4 \times \sqrt{1.8 \times b_{bf} \times t_{bf} \times \frac{Ryb \times Fyb}{Ryc \times Fyc}}$$ *(Provision equation E3-8)*

Where,

t_{cf} = The minimum required thickness of column flange when no continuity plates are provided, inches

b_{bf} = The width of the beam flange, inches

t_{bf} = Thickness of the beam flange, inches

$F_{yb} = F_{yc}$ = Specified minimum yield stress of the beam or column flange, ksi

$R_{yb} = R_{yc}$ = ratio of the expected yield strength of the beam (column) material to the minimum specified yield strength

=1.1, for the ASTM A992 steel beam or column, respectively

$$t_{cf} \geq 0.4 \times \sqrt{1.8 \times 8.30 \times 0.740 \times \frac{1.1 \times 50}{1.1 \times 50}}$$

$1.90 \geq 1.33$ in

OR

$$t_{cf} \geq \frac{b_{bf}}{6}$$ *(Provision equation E3-9)*

$$1.90 \geq \frac{8.30}{6}$$

$1.90 \geq 1.38$ in

Therefore, from both the provisions it is seen that continuity plates are not required.

Step 11: Check beam column beam relationship per ANSI/AISC Section 5.4:

(AISC Seismic design manual page. 4-69, 4-70)

$\frac{\sum M_{pc}^{*}}{\sum M_{pb}^{*}} > 1.0$ *(Provision Eq. E3-1)*

$$\sum M_{pc}{}^{*} = Z_{xt} \times \left[F_y - \frac{P_{uc}}{A_g}\right]\left[\frac{h_t}{h_t - \frac{d_b}{2}}\right] + Z_{xb} \times \left[F_y - \frac{P_{uc}}{A_g}\right]\left[\frac{h_b}{h_b - \frac{d_b}{2}}\right]$$

P_{uc} = 249 kips *(ASIC Seismic Design Example 4.3.2, page. 70)*

$$\sum M_{pc}{}^{*} = 348 \times \left[50 - \frac{249}{61.8}\right]\left[\frac{75}{75 - \frac{21.2}{2}}\right] + 348 \times \left[50 - \frac{249}{61.8}\right]\left[\frac{75}{75 - \frac{21.2}{2}}\right]$$

= 37262.10 kip- in

The expected flexural demand of the beam at the column centerline is defined in ANSI/AISC 358 Section 5.4 as:

$\sum M_{pb}{}^{*} = \sum(M_{pr} + M_{uv})$ *(ANSI/ AISC 358 section 5.4)*

$\sum M_{uv} = (V_{RBS} + V'_{RBS})\left(a + \frac{b}{2} + \frac{d_c}{2}\right)$

= (64.193 kips + 32.263 kips) $\left(5 \text{ in} + \frac{16}{2}\text{in} + \frac{14.7}{2}\text{in}\right)$

= 1962.87 kip-in

Therefore expected flexural demand of the beam at the column center line is:

$\sum M_{pb}{}^{*} = 2 \times M_{pr} + \sum M_{uv}$

= 2 × (7699.67) + 1962.87

= 17362.21 kip-in

$\frac{\sum M_{pc}^{*}}{\sum M_{pb}^{*}} = \frac{37262.10}{17362.21}$ *(AISC Seismic design manual page. 4-71)*

= 2.146 > 1.0 (O.K.)

Therefore, strong-column-weak-beam check is satisfied.

Perform Panel Zone Check

$$V_c = \frac{M_f + M_f'}{\left(\frac{h_t}{2} + \frac{h_b}{2}\right)}$$

$$= \frac{8534.179 + 7280.251}{\left(\frac{75}{2} + \frac{75}{2}\right)}$$

$$= 210.859 \text{ kips}$$

Where,

h_t = Story height above the joint, inches

h_b = Story height below the joint, inches

M_f = Moment at the face of the column, kip-inches

The required strength of the panel zone is:

$$R_u = \frac{\sum M_f}{(d_b + t_f)} - V_c$$

$$= \frac{8534.179 + 7280.251}{(21.2 - 0.740)} - 210.859$$

$$= 562.084 \text{ kips}$$

Where,

V_c = Shear in column due to plastic hinging of the RBS

t_f = Thickness of beam flange

d_b = Depth of the beam

P_r = 243 kips *(AISC Seismic design manual Example 4.3.2, page. 4-72)*

$P_r < 0.75\ P_c$

$P_r < 0.75 \times F_y \times A_g$

$< 0.75 \times 50 \times 61.8$

P_r = 243 kips < 2317.5 kips (O.K.)

Shear strength of the panel zone is given by AISC specification equation J 10-11:

$$\phi R_n = \phi \times 0.6 \times F_y \times d_c \times t_w \times \left[1 + \frac{3 \times b_{cf} \times t_{cf}^2}{d_b \times d_c \times t_w}\right]$$

$$= 1.00 \times 0.60 \times 50 \times 14.7 \times 1.18 \times \left[1 + \frac{3 \times 12.8 \times 1.90^2}{21.2 \times 14.7 \times 1.18}\right]$$

$$= 716.54 \text{ kips}$$

Where,

d_b = Depth of beam, inches

d_c = Depth of column, inches

t_w = Web thickness of column, inches

t_{cf} = Flange thickness of column, inches

b_{cf} = Width of the column, inches

ϕ= 1.00

Alternatively, using Table 4-2 of AISC Seismic Design Manual for W 12×190:

$0.75 \times P_y$ = 2320 kips

ϕR_{v1} = 520 kips

ϕR_{v2} = 4160 kip-in

$\phi R_n = R_{v1} + \phi R_{v2}$

$$= 520 + \frac{4160}{21.2}$$

$$= 716.22 \text{ kips}$$

Since, R_u = 562.084 kips < ϕR_n = 716.22 kips, a column-web doubler plates are not required.

Lateral load calculation for bare steel frame:

From the calculation, the moment on each column face is, M_f = 8534.179 k-in

$$= \frac{8534.179}{12} \text{ k-ft}$$

$$= 711.18 \text{ k-ft}$$

Since, the moment developed on the beam column connection is caused by the column below and above the connection; moment about each column is given as,

$$\frac{M_f}{2} = 355.59 \text{ k-ft}$$

The height of the column above the beam column connection is 6ft and 3 inches.

So, the lateral load is calculated to be:

$$\frac{355.59 \text{ k}-\text{ft}}{6.25 \text{ ft}} = 56.89 \text{ kips}$$

APPENDIX.B

FINITE ELEMENT SOFTWARE (NISA/ DISPLAY IV) OUTPUTS

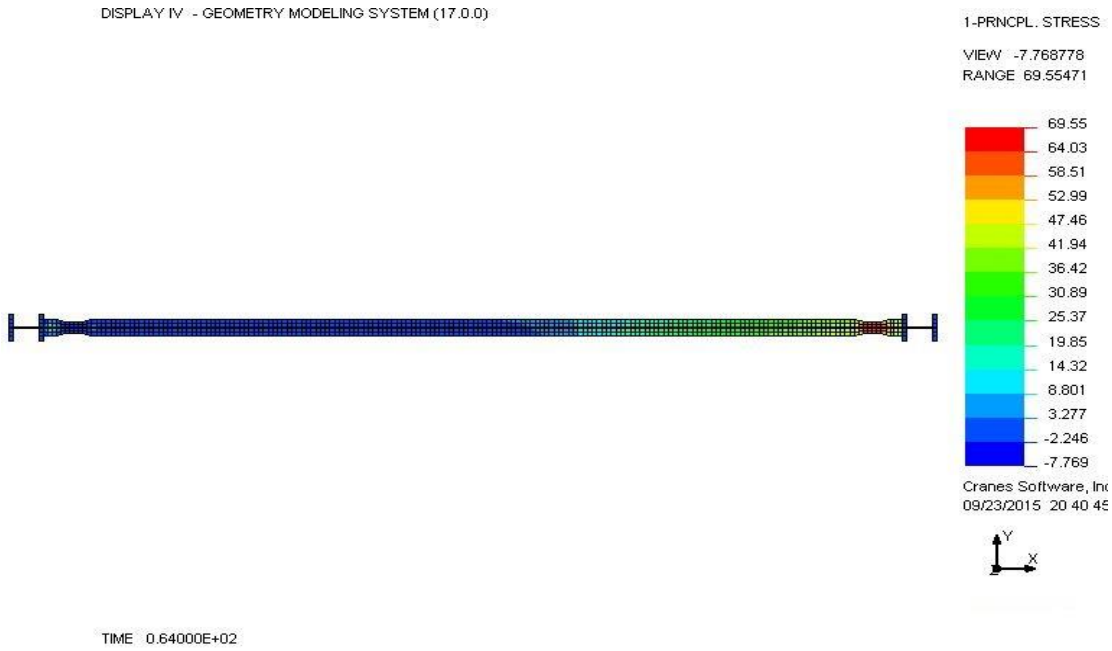

Figure B.1:1st Principal stress top view (Model 1a)

Figure B.2: Von-Mises stress top view (Model 1a)

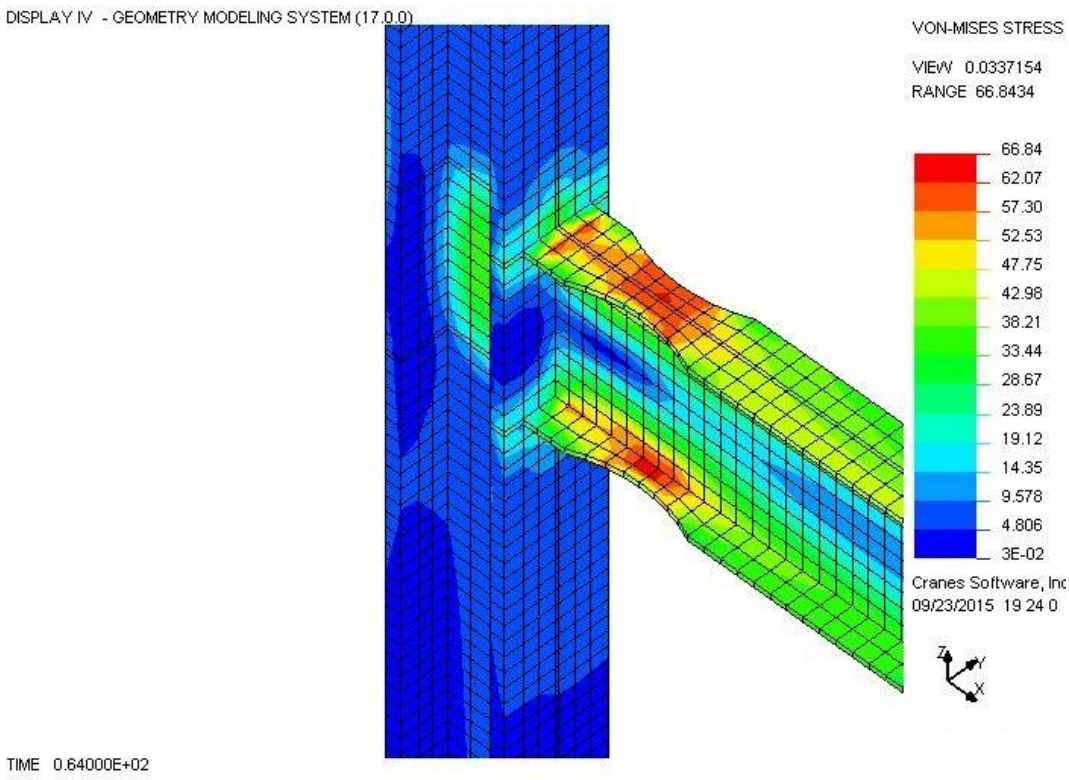

Figure B.3: Plastic hinge formation (model 1a)

Figure B.4:1st Principal stress top view (Model 2a)

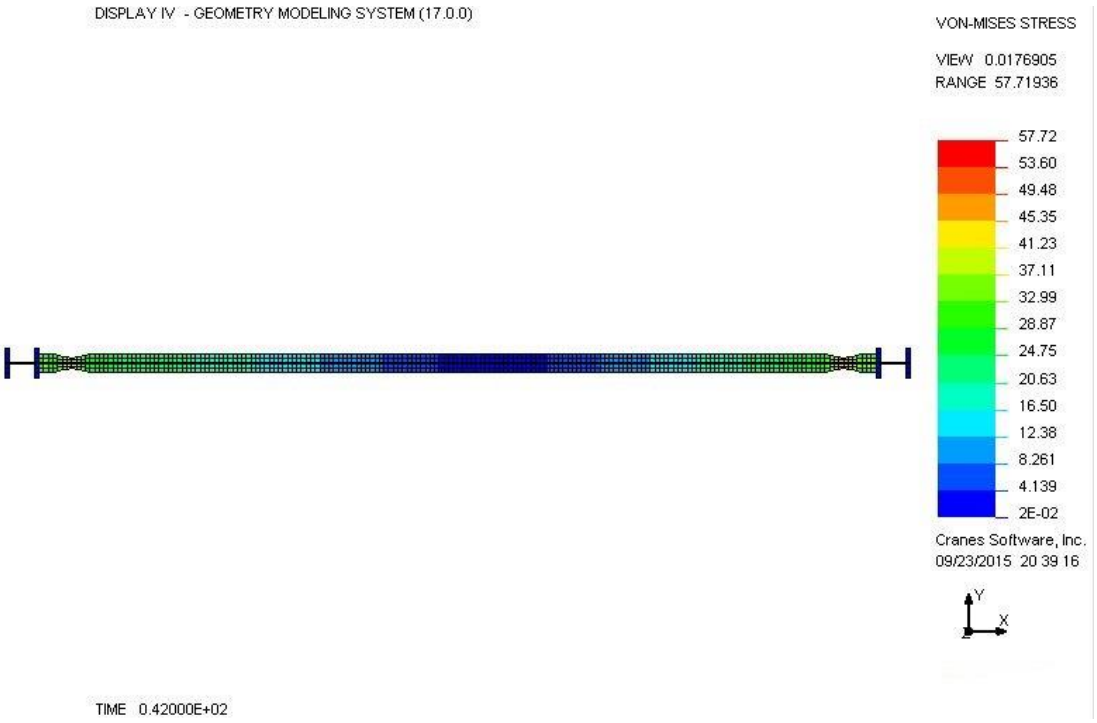

Figure B.5: Von-Mises stress top view (Model 2a)

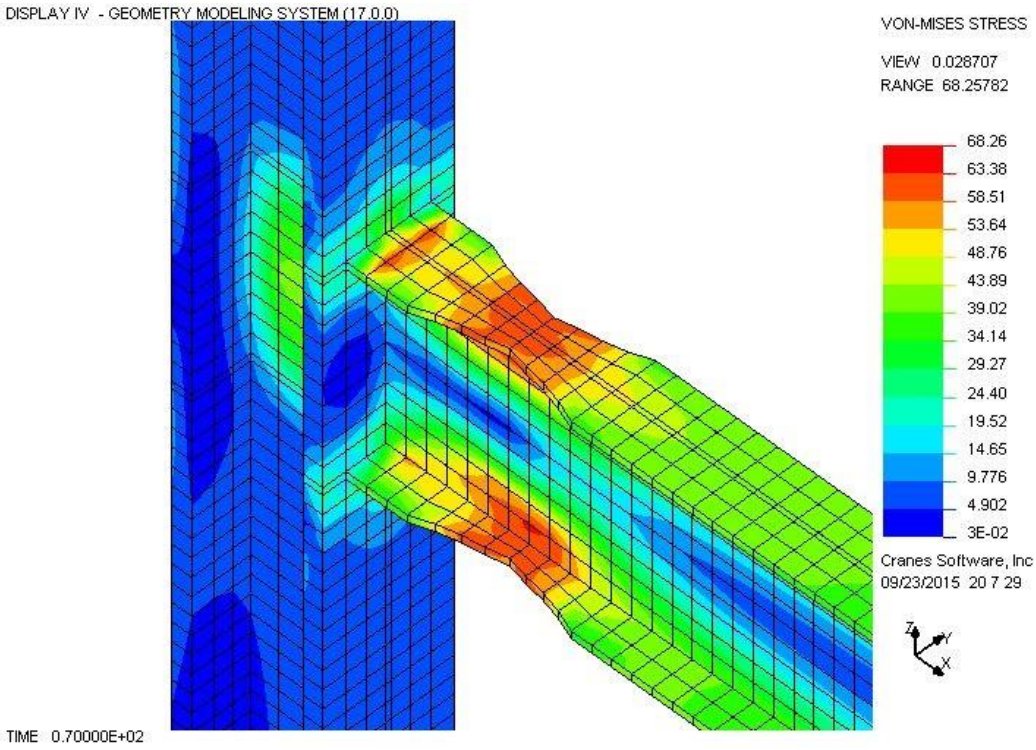

Figure B.6: Plastic hinge formation (model 2a)

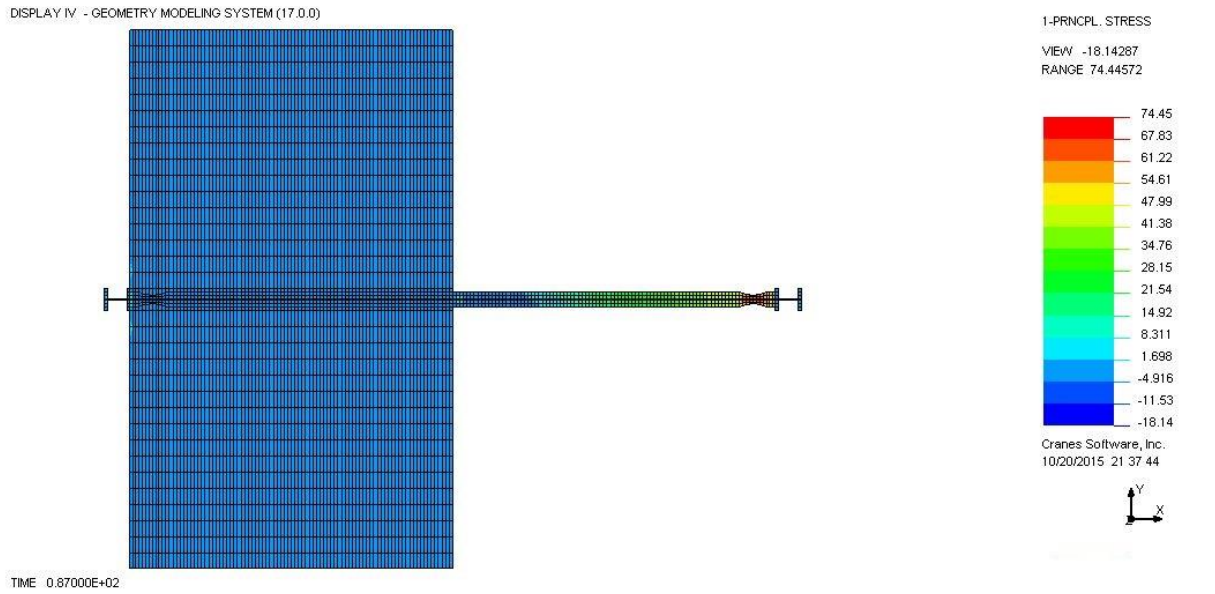

Figure B.7:1st Principal stress top view (Model 1b)

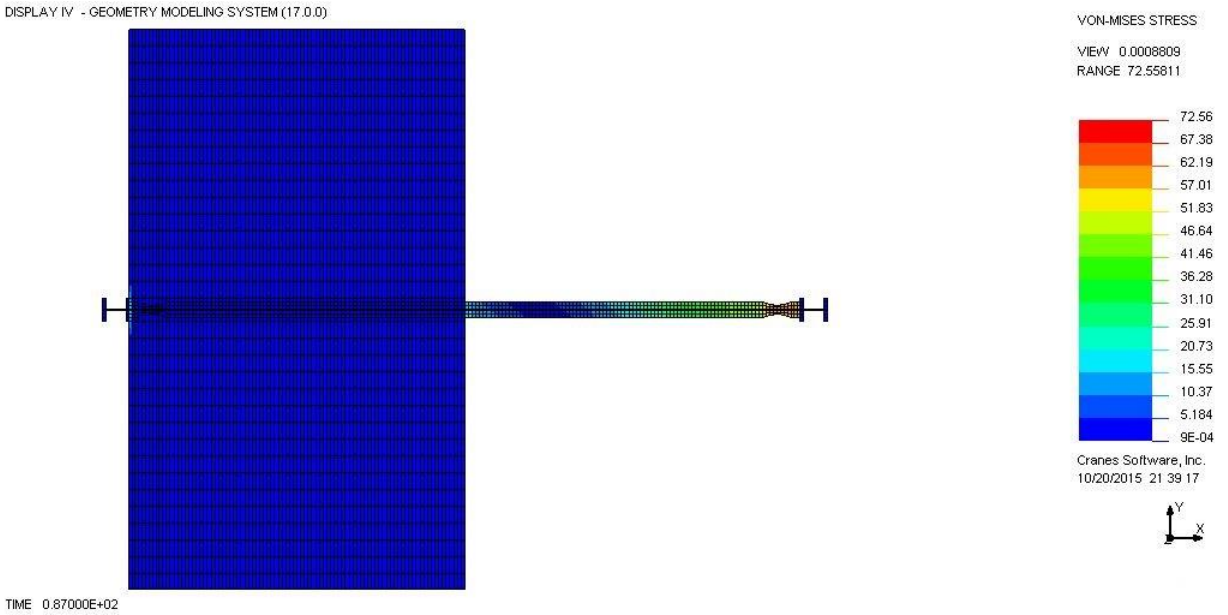

Figure B.8: Von-Mises stress top view (Model 1b)

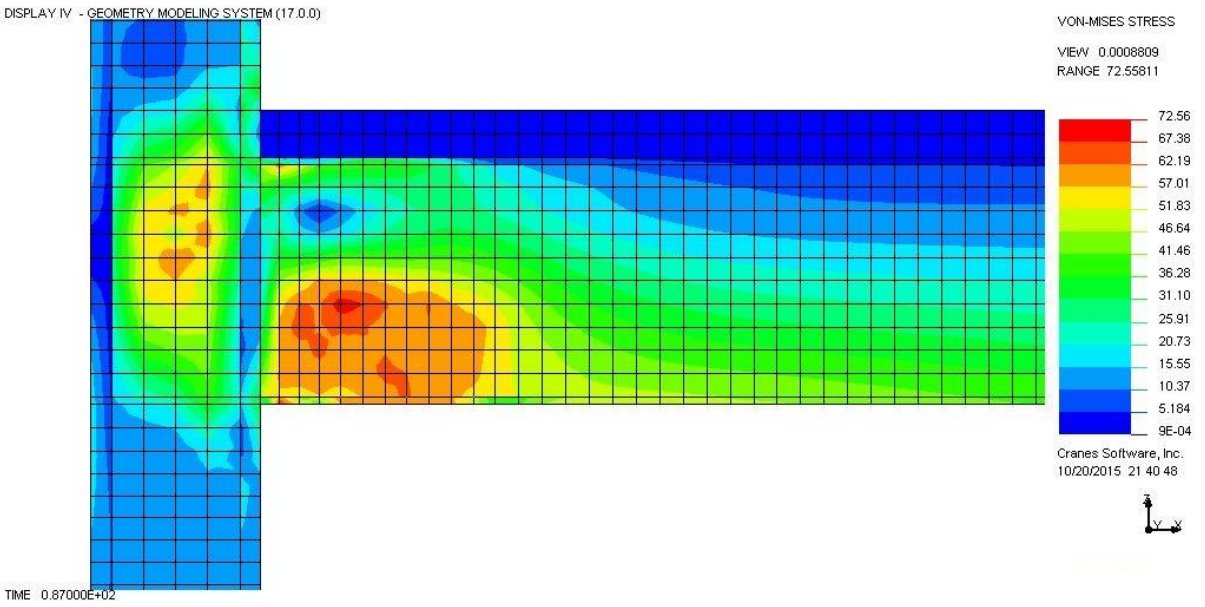

Figure B.9: Plastic hinge formation (model 1b)

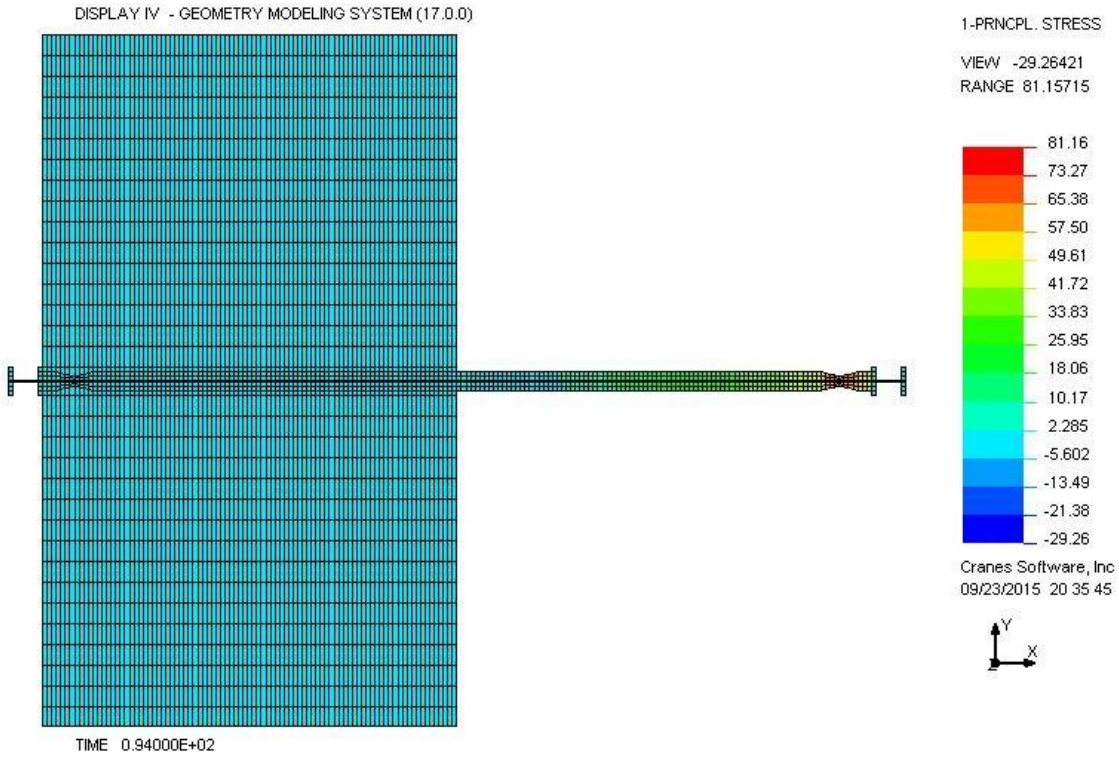

Figure B.10:1st Principal stress top view (Model 2b)

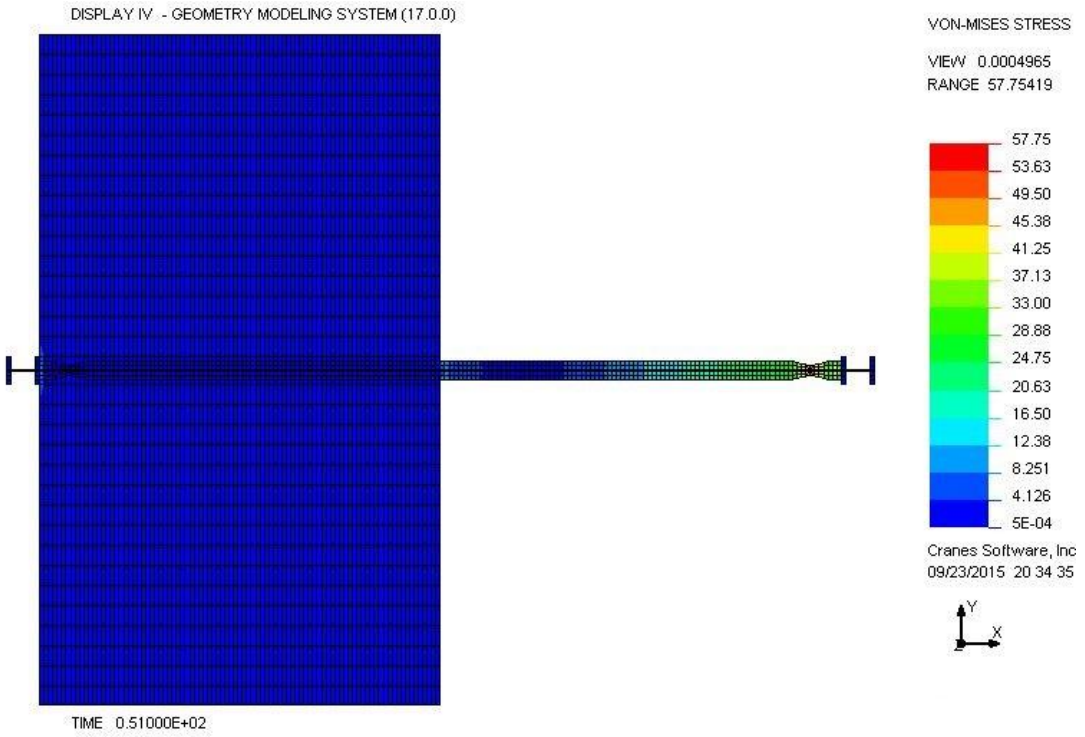

Figure B.11: Von-Mises stress top view (Model 2b)

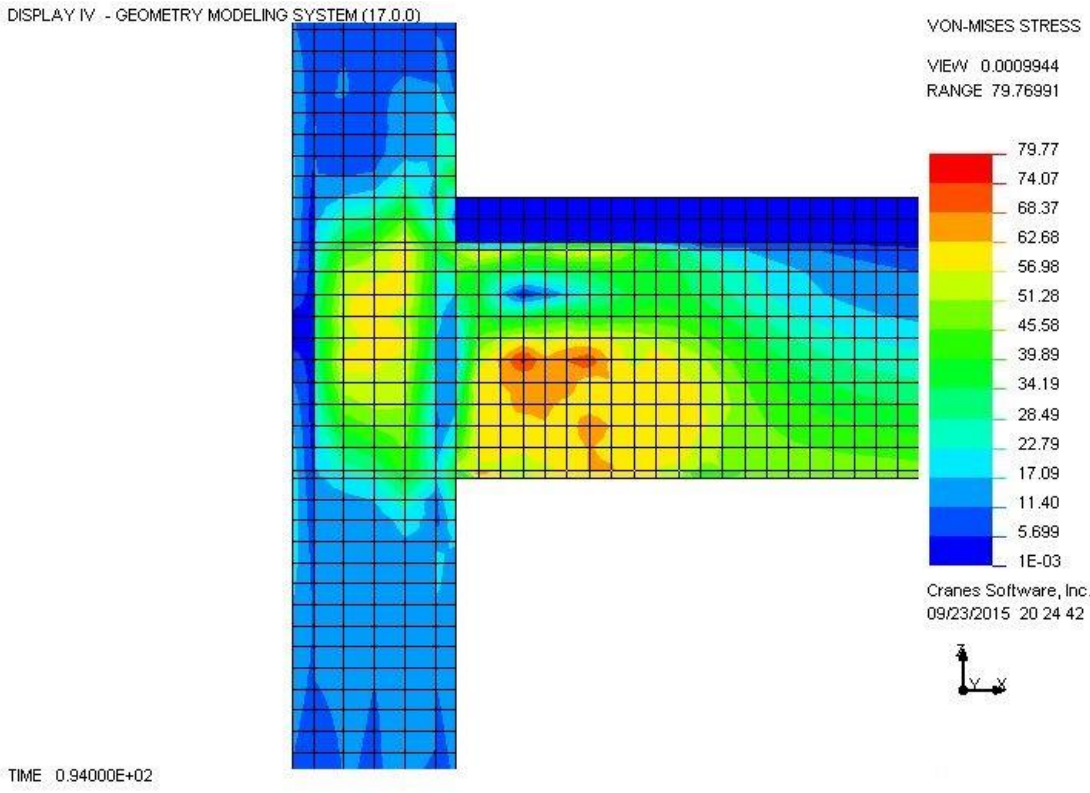

Figure B.12: Plastic hinge formation (model 2b)

Figure B.13: Fracture deformation (Model 1a)

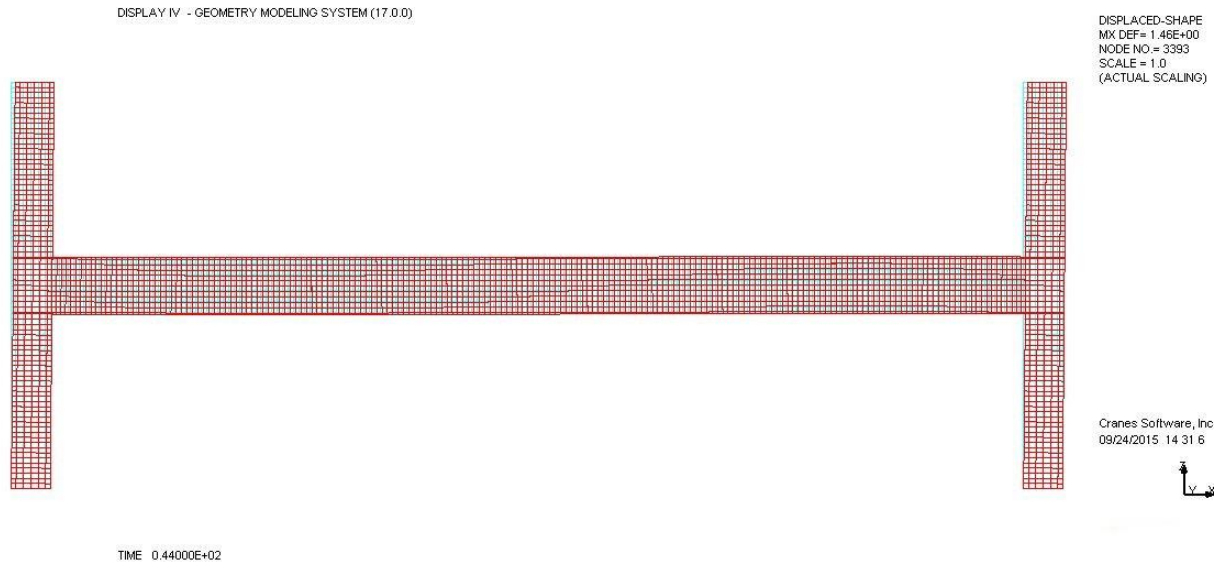

Figure B.14: Yield deformation (model 1a)

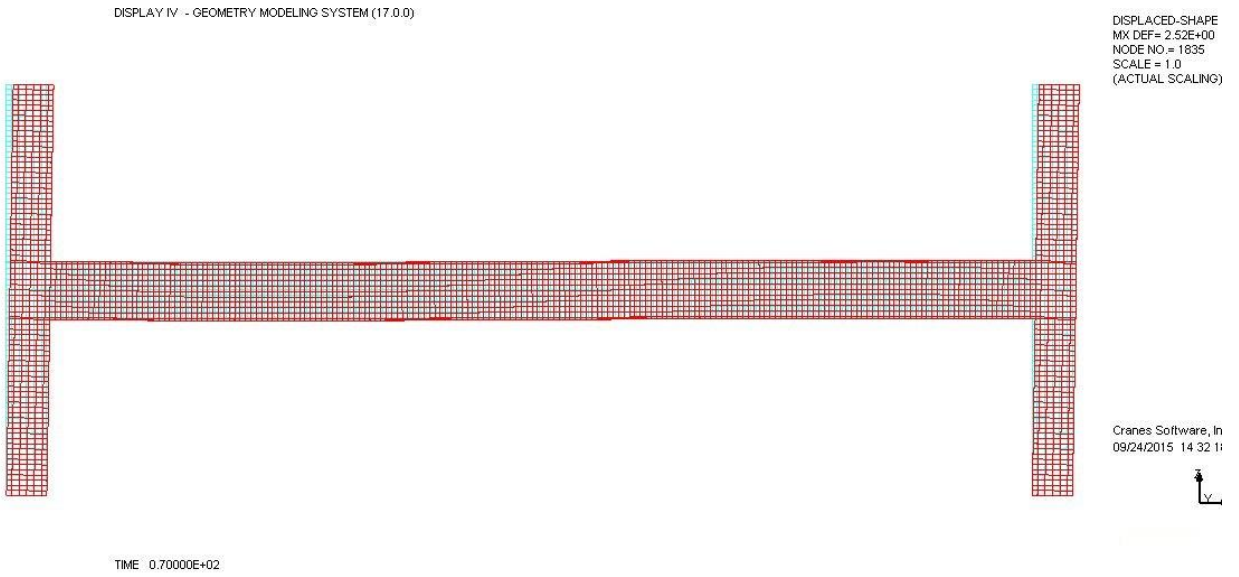

Figure B.15: Fracture deformation (Model 2a)

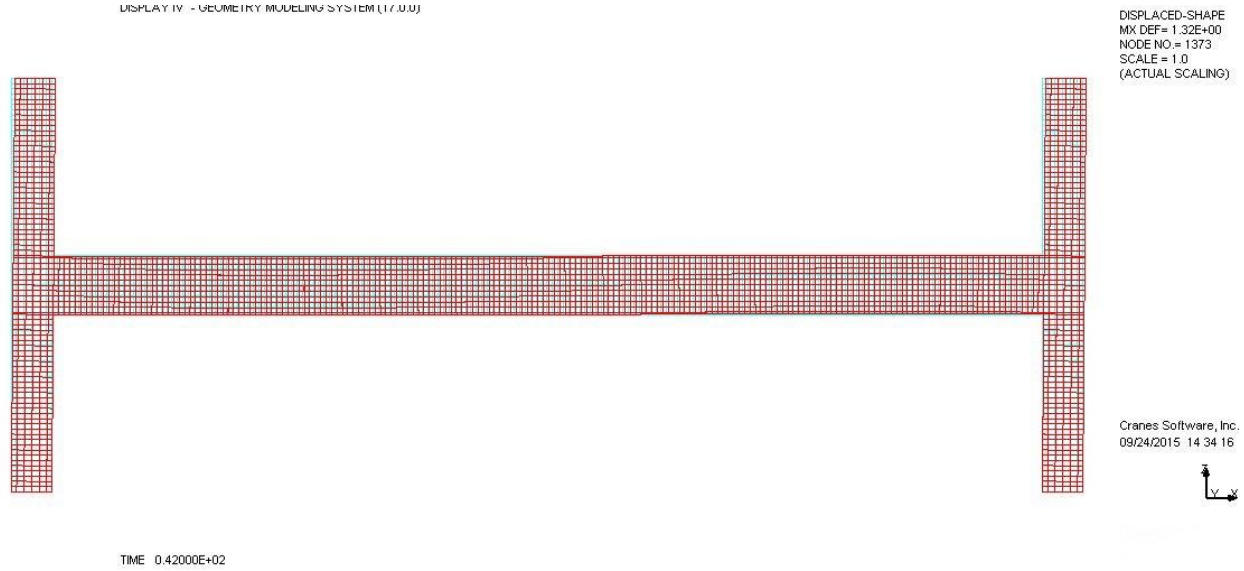

Figure B.16: Yield deformation (Model 2a)

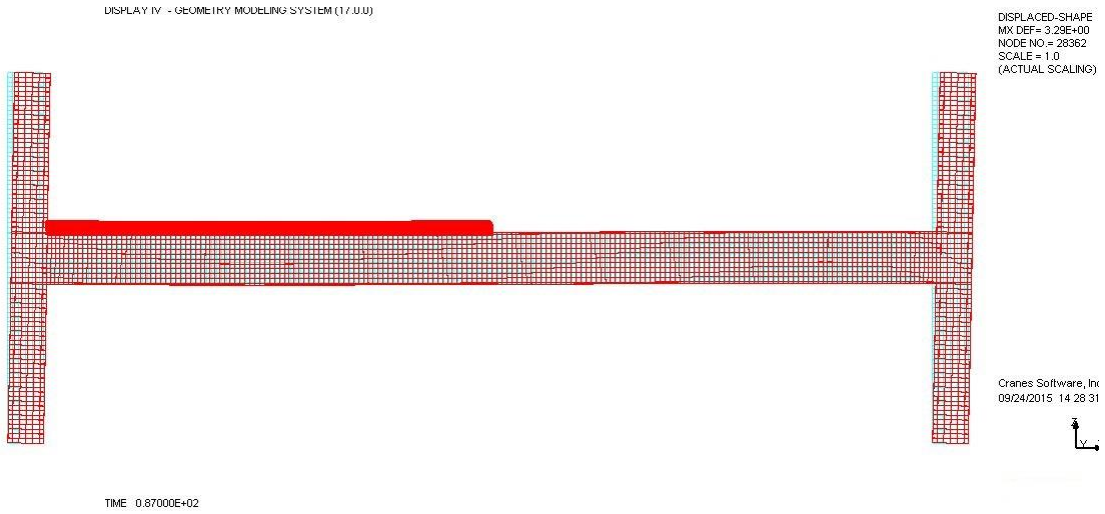

Figure B.17: Fracture deformation (Model 1b)

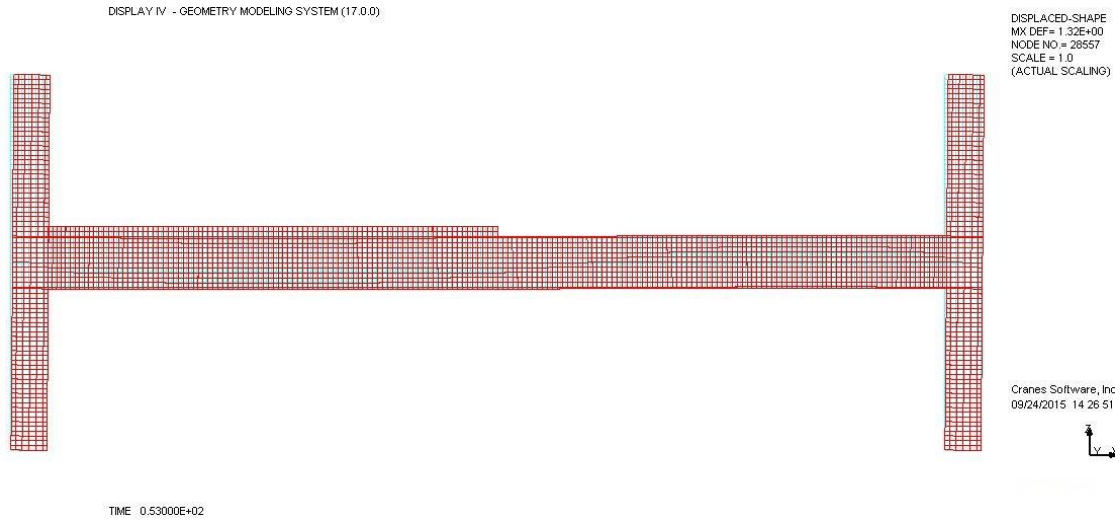

Figure B.18: Yield deformation (Model 1b)

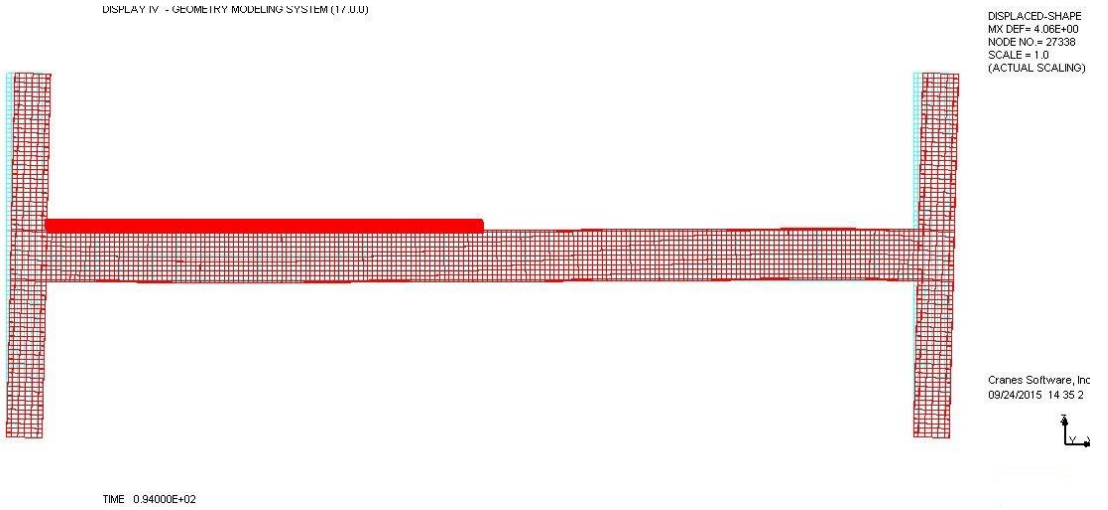

Figure B.19: Fracture deformation (Model 2b)

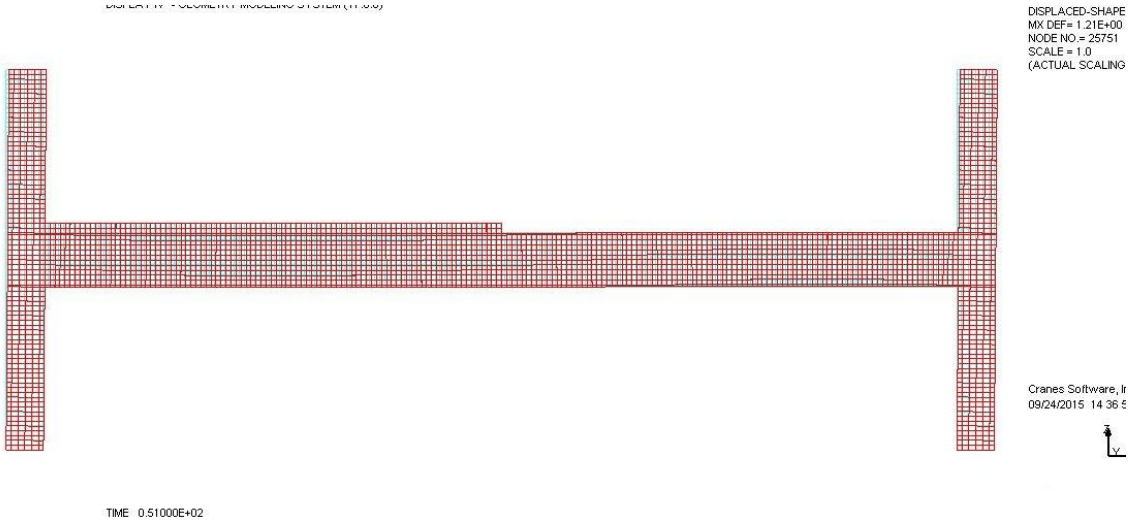

Figure B.20: Yield deformation (Model 2b)

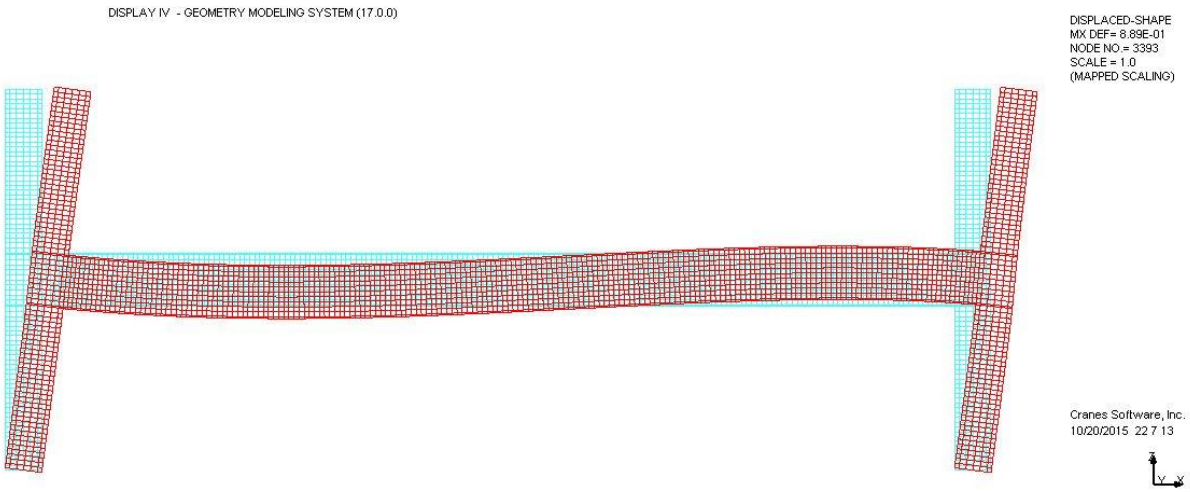

Figure B.21: Elastic deformation (Model 1a)

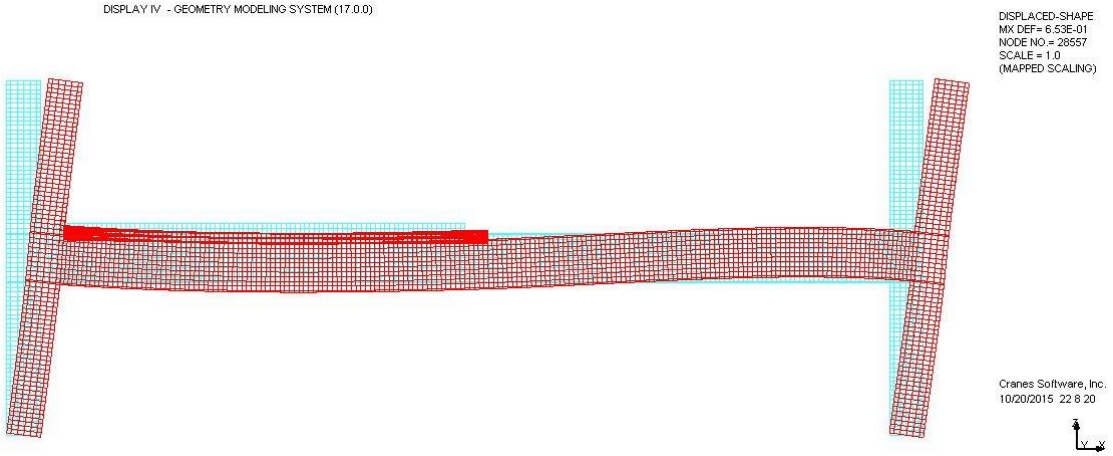

Figure B.22: Elastic deformation (Model 1b)

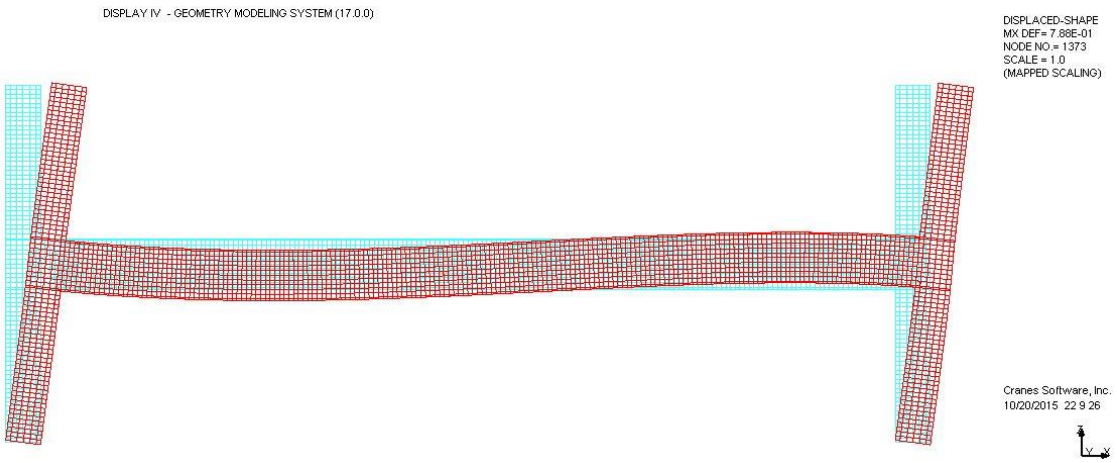

Figure B.23: Elastic deformation (Model 2a)

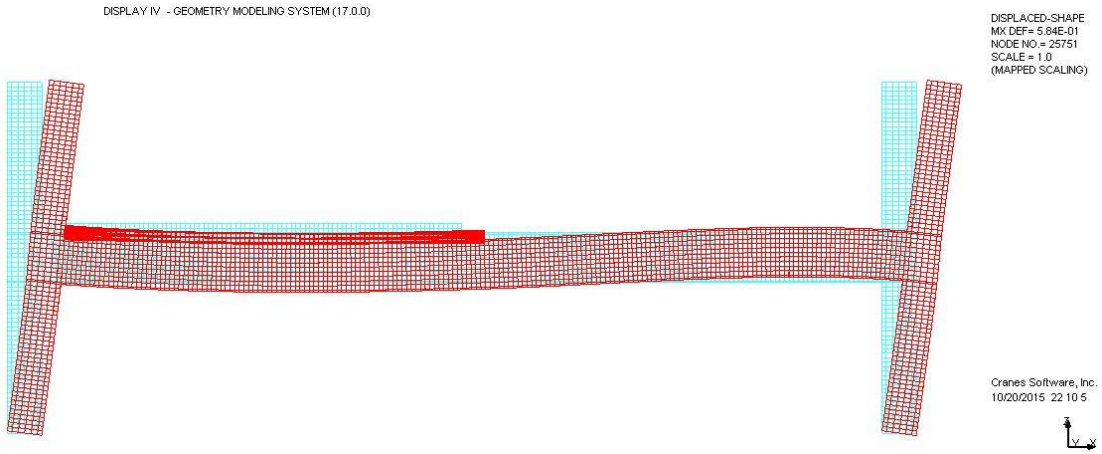

Figure B.24: Elastic deformation (Model 2b)

VITA

Graduate School
Southern Illinois University

Sanchit Poudel
sanchitpoudel@gmail.com

Pulchowk Campus, Kathmandu, Nepal
Bachelor of Science, Civil Engineering, December 2012

Thesis Title:

Effects of Concrete slab on the Ductility, Strength and Stiffness of Steel Moment Frames with Reduced Beam Section Connections

Major Professor: Dr. J. K. Hsiao, Ph.D., P.E. (CA), S.E. (UT)